

Aircraft Conceptual Design Project Report

SAE Brazil Aero Design 2023 - Regular Category

Tarun Teja (tarna588)

Abhishek Dhiman (abhdh352)

Saurav Lal Srivastwa (sausr199)

Aditya Mohan Jaiswal (adija250)

Santosh Raghavendra Yeshwanth (sanna002)

Examiner: David Lundström

Abstract

The report discusses the conceptual designs remote Controlled (RC) plane for the upcoming SAE AeroDesign Brazil Competition, 2023. The team of 5 members (TMAL06 group2) is motivated and dedicated to shape the academic knowledge and skills in form of an RC plane, worthy to participate and hopefully win the SAE competition. Among the three categories, the regular class has a mission profile similar to a civil aviation aircraft i.e to execute take-off with payload, clear the obstacle height, make a 360 [deg] turn, and execute landing with the same obstacle clearance.

The main competition is divided into multiple sub-categories such as **Design** (scored on the technical report, presentation, and media materials), **Flying** (completing mission heats with increasing payload), and a bonus rounds **fast payload removal**. Also, additional bonus points are can be scored by making the RC plane fully electrical since the technological shift towards battery-driven propulsion system aircrafts is impending and has gained significant popularity in recent years.

The work in its entirety is performed under the guidance of Professor David Lundstrom (LiU). Each team member developed its own CAD-generated conceptual design which were later compared and converged into a single design. The individual designs were crucial for evaluating the advantages and disadvantages of different wing plan forms, tail configurations, power-train locations, landing gear positioning and payload placements. Through a comprehensive analysis of all the concepts, the final design had emerged based on their collective merits.

This report takes the reader through steps followed by the team to reach the goal of designing an regular category SAE worthy aircraft and the various analysis performed for the same. It gives an insight of the challenges and problems tackled by the team resulting in final design parameters and CAD model.

Nomenclature

Abbreviations and Acronyms

Abbreviation	Meaning
LiU	Linköping University
SP	São Paulo
CAD	Computer-Aided Design
NACA	National Advisory Committee for Aeronautics
SAE	Society of Automotive Engineers
FCS	Flight Control Systems
RC	Radio Controlled
MTOW	Maximum Take Off Weight
AoA	Angle of Attack
CG	Center of Gravity
NP	Neutral Point
SM	Static Margin
TO	Take Off Distance
LD	Landing Distance
RCA	Regular class Aero design

Abbreviations and Symbols

Symbol	Description	Units
S_{ref}	Reference Area	[m^2]
MAC	Mean aerodynamic chord	[m]
b	Wing span	[m]
AR	Aspect ratio	[NA]
λ	taper ratio	[NA]
α	Angle of attack	[degree]

Contents

1	Introduction	6
1.1	Project Description: Mission overview	6
2	SAE Requirements & Studies	7
2.1	SAE Operating Constraints	7
2.2	Former SAE Participants	7
2.3	SAE Regulations	8
2.4	Inspiration	8
3	Design Goal and Requirements	9
3.1	Mission Profile	9
3.2	Design Requirements	9
4	Concepts and Selection Process	11
4.1	Individual Conceptual Design (MS2)	11
4.1.1	Santosh Raghavendra Yeshwanth (sanna002) Concept 1:	11
4.1.2	Tarun Teja (tarna588) Concept 2:	13
4.1.3	Saurav Lal Srivastwa (sausr199) Concept 3:	15
4.1.4	Aditya Mohan Jaiswal (adija250) Concept 4: & Abhishek Dhiman (abhdh352) Concept 5:	17
4.2	Concept Selection Process (MS3)	20
4.3	Individual Concepts Convergence	21
4.4	Final CAD Design (MS4)	23
4.5	Finalized Concept: Detailed CAD Model	26
4.6	Final Design Sizing Diagram	32
5	Aerodynamic Analysis	34
5.1	Airfoil Performance	34
5.2	Drag Polar	34
6	Performance Analysis	39
6.1	Takeoff (TO) and Landing (LD)	39
6.1.1	Takeoff (TO)	39
6.1.2	Landing (LD)	40
7	Stability and Control Analysis	43
7.1	CG Estimation	43
7.2	Neutral Point (NP) and Static Margin (SM)	44
8	Loads and Aero Elasticity	46
8.1	Payload and Dimension Analysis	46
8.2	Component Selection and Weight	47

9 Structures and Structural Test	48
9.1 Aircraft Structures and Weight Estimation	48
9.2 Lifting Surfaces	48
9.3 Fuselage	49
9.4 Landing Gear	49
10 SAE: Additional Analysis	50
10.1 Control Analysis	50
10.2 Aero Elasticity	50
10.3 Material Table and Structural Tests	50
10.4 Electrical Design and Safety Assessment	50
11 Conclusion and Future Scope	50

List of Figures

1 Design Analysis of former SAE participants	7
2 Mission for Regular category [1].	9
3 Concept1: Oblique view show salient features	12
4 Concept1: Side view show payload placement	12
5 Concept1: Top view	12
6 Concept2: Oblique view show salient features	14
7 Concept2: Side view	14
8 Concept2: Top view with fuselage profile	14
9 Concept3: Oblique view show salient features	16
10 Concept3: Side view	16
11 Concept3: Top view with fuselage profile	16
12 Concept4: Oblique view show salient features	18
13 Concept4: Side view	18
14 Concept4: Top view with fuselage profile	18
15 Concept5: Oblique view show salient features	19
16 Concept5: Side view	19
17 Concept5: Top view with fuselage profile	19
18 Scoring Matrix Of Concept Selection Process	20
19 Concept2: Oblique View	21
20 Concept6: Work in progress	21
21 Concept6:Work in progress with variable payload placement	22
22 Isometric view for the first design	24
23 Top view for the first design	24
24 Side view for the first design	24
25 Isometric view for the second design	25
26 Top view for the second design	25
27 Side view for the second design	25
28 Top view of the finalized model	26
29 Side view of the finalized model	27
30 Front view of the finalized model	27

31	Bottom view of the finalized model	27
32	Isometric view of the finalized model with full payload 10 [kg]	28
33	Internal structure of the finalized model wing and tail	28
34	Skeletal structure of the finalized model	28
35	Internal section for the electric components and the payload	29
36	Payload comprising of stainless steel plates, weight range [5-10] kg . .	29
37	Payload comprising of stainless steel plates, weight range [5-10] kg . .	29
38	Servo locations on the wing for ailerons	30
39	Servo locations on the vertical tail for rudder	30
40	Servo locations on the horizontal tail for elevator	30
41	Finalized draft of the model with specific dimensions	31
42	Constraint Diagram	33
43	C_l/C_d and C_l vs C_d Graphs	35
44	Airfoil Comparison Graphs	35
45	Total Drag graph	37
46	Drag Polar	38
47	Takeoff Stages [2]	39
48	Landing Stages [2]	40
49	Stall velocity (V_s) variations in LiU and Sau Paulo (Brazil) elevations	41
50	Take off and landing distance affected by payload increment	41
51	Temperature influence on Take distance in Linkoping and Sau Paulo	42
52	Temperature influence on landing distance in Linkoping and Sau Paulo	42
53	Individual component and Aircraft CG	43
54	Comparison of term values for X_{NP} with reference	44
55	Aircraft CG and NP location w.r.t MAC	45
56	Payload and payload compartment dimension analysis	46
57	Component dimensions and weight	47
58	Weight Breakdown of Individual Components	49
59	Individual Weight Distributions of components	49

1 Introduction

The Society of Automotive Engineers has been conducting an Aeronautical Design competition in Brazil since 1999 which is considered to be best place for aspiring aeronautical engineers to compete and show their Aeronautical skills & Knowledge. The Competition is organized in two stages, the Design Competition and the Flying Competition along with a bonus round like fast removal of payload [1].

The SAE Aero Design Competition has been conducted in the United States since 1986, having been conceived and carried out by SAE International, a company that gave rise to the SAE BRASIL in 1991 year. Since 1999 this competition has been included in the SAE BRAZIL student events calendar. The models or projects in Aero Design (BRAZIL) over the years have made immense growth in terms of quality and strength of participation. This growth is also reflected in each and every participant through significant learning and professional training gained in the process. The Technical Committee of this competition always had one of its main objectives building technical sharpness, professionalism and enhancing the teamwork capabilities in the participants which is the fundamental requirement in the field of Engineering Science [1].

There are 3 Sub-categories from which the teams can choose to compete, namely **Micro, Regular, and Advanced** classes. This allow the teams to design the RC Aircraft and complete the mission for the class of their choice. Each class has its own scoring structure and several aspects are considered to get higher score. The Aero Design competition offered to students in graduate and under graduate level of university. Main objective of this competition is that each team must conceive, design, document, build and fly the RC airplane which is optimized in all design aspects. Following sections present the detailed explanation of thorough analysis conducted by the team which to optimize the aircraft conceptual design and eliminate the scope of failures as much as possible.

1.1 Project Description: Mission overview

The team has selected to participate in the Regular class, which is going to be discussed in this report. The Regular class RC airplane design with the utilization of an electric motor-driven propulsion system accounts for an additional 50 points. The designed aircraft needs to carry a varying payload in the range [5, 7, 9, 10] kg (**weight increment with successive heats**) and clear an obstacle height of 70 [cm] and width of 10 [m]. The total runway for take-off and landing is 110 [m], dedicated to 55 [m] for take-off, and the same for landing, Fig. 2. The mission is to execute the take-off, clear the obstacle placed on the opposite end of the runway, make a 360 [deg] turn, and perform the landing. There are a total of 7 heats in which the aircraft must clear the mission without the Payload in heat [1, 2, 3] and on the 4th heat the aircraft must carry the 5[kg] payload and clear the mission. For subsequent heats the payload will increase reaching a maximum value of 10[kg] on the final heat. The details of mission profile and bonus rounds for gaining higher score are discussed in following section.

2 SAE Requirements & Studies

2.1 SAE Operating Constraints

The requirements are mentioned in detail in [1], the gist is mentioned below with the section number.

- R[7.5.2.2] Single compartment payload, **must not** contain lead parts.
- R[7.3.2.9] Motor - Electric Motor utilization (50 points)
- R[7.2.0.1] Fixed Wing, Wing Span (S) ≤ 2.3 [m], Height (H) ≤ 0.6 [m]
- R[7.3.2.1] Power Train (P_t) ≤ 700 [W]
- R[7.6.2.1] Propulsion Battery - Battery ≥ 3000 [mAh]
- R[7.6.2.2] Number of Cells in Battery (N) ≤ 6
- R[6.12.1.1] Battery - Lithium Iron Polymer [LiFePO4]
- R[6.11.0.1] Radio Frequency - 2.4 [GHz]
- R[7.7.0.1] Maximum take off Weight (MTOW) ≤ 20 [kg]

2.2 Former SAE Participants

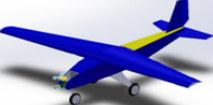
Concepts	FIU, 2014 SAE Brazil	FAMU-FSU, 2020	U Arizona, 2013	Concept4
Reference Designs				
span [m]	2.100	1.800	2.260	3.600
height [m]	0.700	0.730	0.650	0.800
span/height	3.000	2.466	3.477	4.500
Landing gear	Tricycle	Tricycle	Taildragger	Tricycle
Airfoil	Eppler E423	Eppler E423	S1223	NACA-0009
Comment	-	Observed crash landed due to Unstable moments	-	Tail heavy and handling issues

Figure 1: Design Analysis of former SAE participants

The design report [3], [4] and [5] of former SAE participants and the youtube videos uploaded by them encompasses the major portion of the literature survey. The primary objective was to obtain the RCA dimensions and issues faced but the teams during flight tests. The team [4] constructed their own airfoils, expecting better performance but post-analysis and considering the manufacturing difficulties ended up using Eppler 423, Fig. 1. Most of the designs had the combined length of wing span and total vertical height of the aircraft below or around 2.9 [m] as per SAE requirements [1]. The main issues observed were with the weight distribution and tail heaviness leading to the crash landing in the initial test flights.

2.3 SAE Regulations

- **Wing** - The wing should have a maximum span of 2.3[m] and be completely rigid meaning the wing should not have any moving parts if any moving parts are identified the team will be disqualified.
- **Engine** - An electric motor is chosen since it carries a 50-point advantage in the competition and also is a sustainable option. The number of engines used in the design is restricted to **one**. A removable device-style arm plug to activate or deactivate the supply of the engine must be used for an Electric motor.
- **Battery** - The battery to be used is a Lithium Polymer or Lithium Iron Polymer(LiFePO₄) with a minimum energy of 3000[mAh].The number of cells used in the battery should be a maximum of **6** and the battery should have a maximum discharge rate of 20C.
- **Power Train** - A power train consists of the Motor, Battery, Flight control systems, and a watt-meter which combined should have a power of up to 700 [W].
- **Flight control systems** - The FCS should have a dedicated battery and must not use Lithium-ion Polymer[LiPO] hence a Lithium Iron Polymer(LiFePO₄) with a minimum energy of 500[mAh] is being used and also the servos present in the FCS should be commercially available.
- **Payload** - The Payload can be of the team's own choice but the payload should be a sum of the weights of the plates (or load) plus the load support and the team chose to go with **Stain-less steel metal plates** considering its high density and low cost. The Payload compartment dimensions and the volume is of the team's choosing but it should be a single compartment.
- **Propeller** - The propeller for the engine must be commercially available and if the team chooses a specially designed propeller it should be specifically done by the team and a report must be sent to the SAE Brazil committee which reviews the design and takes a decision on the use of the propeller. The Only restriction on the propeller is the ban on Metal propellers due to the dangers of physical harm caused by metal propellers.

2.4 Inspiration

The fundamental inspiration comes from the lack of participation in academic competitions for most of the team members. Leading to curiosity and the impending adventure that SAE AeroDesign offers. Putting theoretical knowledge into the structured product development process stages **[requirements, planning, design, development, test, and deployment]** accelerates the dedication required. Finally, the opportunity to represent the LiU (Linkoping University) on a world platform is a certain delight and puts great responsibility on the team.

3 Design Goal and Requirements

3.1 Mission Profile

Fig. 2 shows the mission that the team needs to carry-out. Initially the plane is placed at the white starting point which is 55[m] from the obstacle the plane needs to generate enough lift to cross the obstacle without damaging it. The obstacle is 0.7[m] high and 10[m] wide. Once the aircraft is in air it needs to do a 360deg turn and clear the obstacle placed on the other end of the runway and start to land. While landing the aircraft must not damage the obstacle. Once the landing is started the landing gear must touch the runway before the white starting point and must not cross the white starting point. This mission is carried out for 9 heats in which the first four heats are carried out without any payload of 5[kg] in the fifth heat and correspondingly increasing the payload with successive heats finally reaching a payload of 10[kg] in the final or ninth heat.

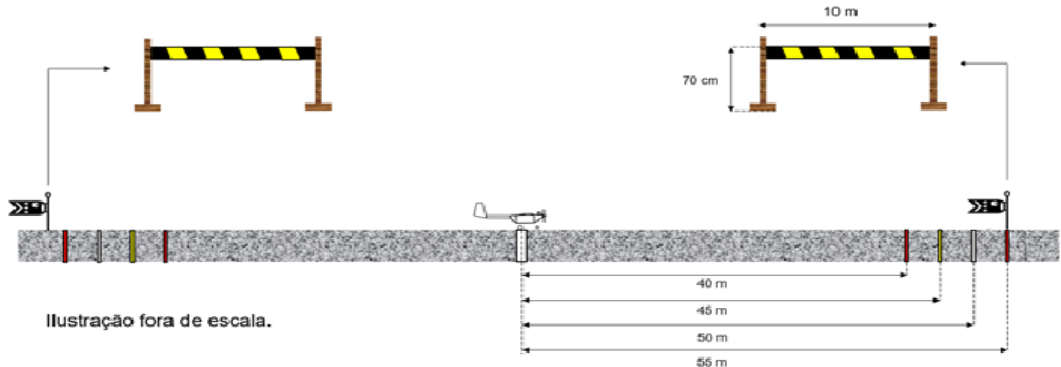


Figure 2: Mission for Regular category [1].

3.2 Design Requirements

The SAE Aero Design Regular Category RCA mission requires the aircraft to take off from a 55 [m] runway, clear an obstacle with a height of 0.7 [m] and a width of 10 [m], execute a 360 [deg] turn, and land within 55 [m] on the same runway while crossing the same obstacle. The total aircraft height (from ground to rudder tip) and span (b) should not exceed 2.9 [m] (R[7.2.0.1]) [1].

The initial set of specifications is tabulated in Fig. 3. The S1223 airfoil is selected for high chamber and good lift generation at low speeds and low angle of attacks (α). Even though the airfoil is hard to manufacture the advantages of the airfoil outweigh the disadvantages. The sum of span (b) and the total aircraft height (from ground to rudder tip) are restricted to be 2.9 [m] (R[7.2.0.1]) [1], hence to achieve the good aspect ratio (AR = 5.5), the span is fixed to 2.3 [m]. This also gives room for large landing gear and a rudder of 0.9 [m]. The fuselage dimensions ($1.89 * 0.075 * 0.075 [m^3]$) are influenced by the payload dimensions as well as the tail positioning to achieve high in-flight stability with a long lever arm for the horizontal stabilizer.

The slenderness ratio achieved is 8.34 which is closer to the upper limit of a good range of 6-8 for sub-sonic flights [6].

High-Level technical Specifications

Design Parameters	Value	Units
Wing span	2.300	[m]
Mean Aerodynamic Chord (MAC)	0.417	[m]
Wing Root Chord	0.500	[m]
Wing tip chord	0.300	[m]
Root thickness Chord ratio	0.121	[NA]
Reference Area	0.965	[m ²]
Aspect Ratio	5.500	[NA]
Fuselage + Boom Length	1.690	[m]
Boom Diameter	0.020	[m]
Fuselage Width	0.09	[m]
Fuselage Nose Width	0.065	[m]
Fuselage Tail Width	0.055	[m]
Horizontal Tail Span	0.900	[m]
Horizontal Tail MAC	0.220	[m]
Horizontal Tail Root Chord	0.250	[m]
Horizontal Tail Tip Chord	0.190	[m]
Elevator Width	0.055	[m]
Vertical Tail Height	0.297	[m]
Vertical Tail MAC	0.220	[m]
Vertical Tail Root Chord	0.300	[m]
Vertical Tail Tip Chord	0.140	[m]
Winglet Angle	20	[deg]
Winglet Chord Length	0.100	[m]
Winglet Height	0.200	[m]
Payload Compartment Length	0.500	[m]
Payload Compartment Diameter	0.100	[m]
Propeller(2 Blade) Diameter	0.381	[m]

4 Concepts and Selection Process

4.1 Individual Conceptual Design (MS2)

4.1.1 Santosh Raghavendra Yeshwanth (sanna002)

Concept 1:

The design approach is based on conventional RC planes with a simple design of rectangular fuselage cross-section and a rectangular wing with a conventional tail design which provides adequate stability and control. The rectangular fuselage cross-section is chosen due to its simplicity in construction and good structural integrity also all the rectangular volume can be used for payload and avionics which is not the case for circular cross-sections also keeping in mind the mission that needs the aircraft to carry payload incrementally the rectangular cross-section provides a good volume for incrementally adding the loads. The Rectangular wing is structurally Strong and capable of carrying heavy loads. It is easy to manufacture. The wing is placed in a High wing configuration to have better stability and also helps in landing. The airfoil used is a NACA4421 which is a thick airfoil with a chord of 0.4 [m] Fig. 4, The span of the wing is 2.3 [m] Fig. 5. A similar Airfoil and Wing shape is used for the Vertical Stabilizer but the location of the vertical stabilizer is at the center of the aircraft to help in landing and take off. The wing is placed at 0.5 [m] from the front of the fuselage.

The landing gear used is a Tail wheel type fixed having the landing gear in front of the CG, This helps in rough and uneven landings distributing the weight of the aircraft evenly which helps less stress on the structure of the airplane. This landing gear is inspired by crop dusters and sailplanes which are more suitable for taking off with a good amount of payload and landing safely in a small area.

The electric motor is placed at the front of the aircraft where propellers can be mounted and the battery for the motor is placed behind the electric motor to evenly distribute the load Also due to the length of the fuselage placed the battery in the front part will not make it too front heavy. The propellers used are 19-inch 3 propellers. The big propellers can generate thrust which can carry the required MTOW of 20 [kg].

The Payload compartment is placed under the wing closer to the CG and the compartment extends until the back landing gear. It is placed in such a manner to avoid making the front part of the aircraft too heavy thereby making the aircraft tip over while landing.

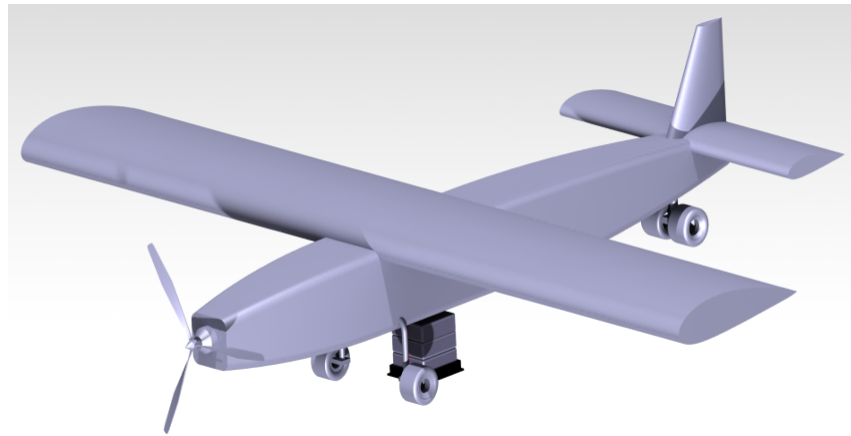


Figure 3: Concept1: Oblique view show salient features

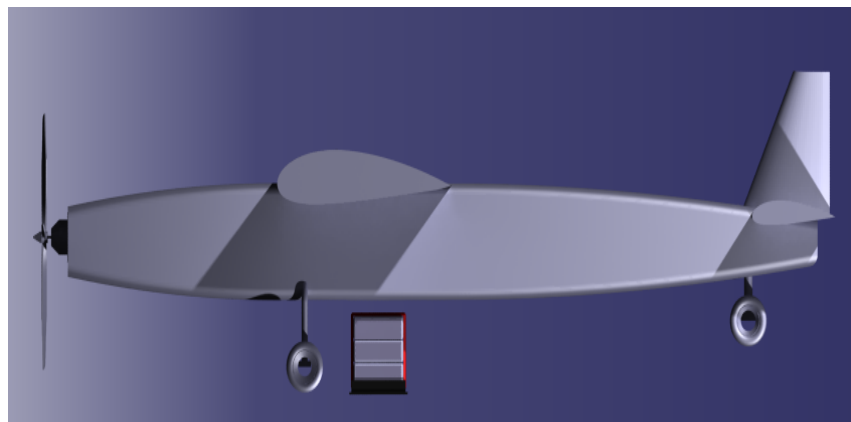


Figure 4: Concept1: Side view show payload placement

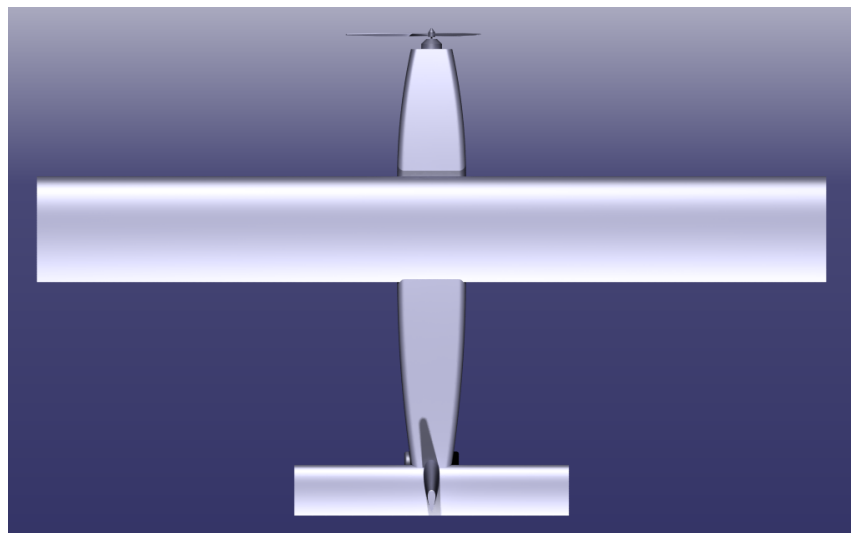


Figure 5: Concept1: Top view

4.1.2 Tarun Teja (tarna588) Concept 2:

The choice of twin-boom aircraft concept is acknowledged keeping the geometry constraints for SAE competition, the design is galvanized from De-Haviland Vampire(DH 100 Vampire) aircraft which was first flown on 20th September 1943, the twin-boom configuration has a shorter fuselage housing the payload and supports the other structures like tail surfaces and acquired to solve the various problems having with conventional empennage configuration for Remote control airplanes.

The Fuselage configuration is a super-elliptical cross-section that is used to carry both the Payload 5 [kg] and the Batteries of the airplane which gives more flexibility in using interior design space and perfectly complements the twin-boom aircraft. This results in the potential enhancement of aerodynamic performance which is the prime provision during the mission of the competition. The amount of lift distribution will be equal all along the wing and will have the same effective Angle of attack over the wing span. On the downside, the twin-boom generally offers greater drag compared to conventional aircraft for a purpose of that elliptical-shaped fuselage, Fig. 7.

The Trapezoidal wing configuration befits the twin-boom aircraft which provides low-aerodynamic drag at low speeds and maintains a high strength-to-stiffness ratio. The span loading of the wing between two booms can reduce structural forces and makes aircraft lighter and smaller. The geometry of the wing span is 2.3 [m] and the chord is 0.4 [m]. The airfoil used for the wing, the horizontal stabilizer, and the vertical stabilizer is NACA-4421. NACA 4421 thickness will enhance the structural property of the wing resulting in increased overall aerodynamic performance. On the other hand, the shape of the horizontal stabilizer is kept rectangular. The horizontal stabilizer is high-mounted on twin tail fins and the two outboard tails clear the airframe of the propeller blades of the engine motor. The tail is supported at both ends of the airplane Fig. 6 The two vertical stabilizers provide additional stability and control in the Yaw axis during take-off, cruise, and landing compared to conventional airplanes.

The single Engine (Electric motor) with a propeller located at the rear end of the fuselage in the pusher configuration, a conventional tail requires a very long power draft which results in a reduction of propulsion efficiency but a twin-boom configuration allows a shorter and most efficient installation.

The primary function of landing gear is to reduce the substantial impact forces and moments while transferring them safely into the air-frame. The configuration of the landing gear is tricycle is kept as fixed rather than retractable which allows dynamic stability on the ground and easy maneuverability. This aids in the SAE competition as this configuration, particularly in the mission has good control over crosswinds and protects the propeller from striking the ground. It is easier to land as well as forgiving for inexperienced pilots during competition, as it also has a lesser bounce-back effect after a touchdown, Fig. 7.

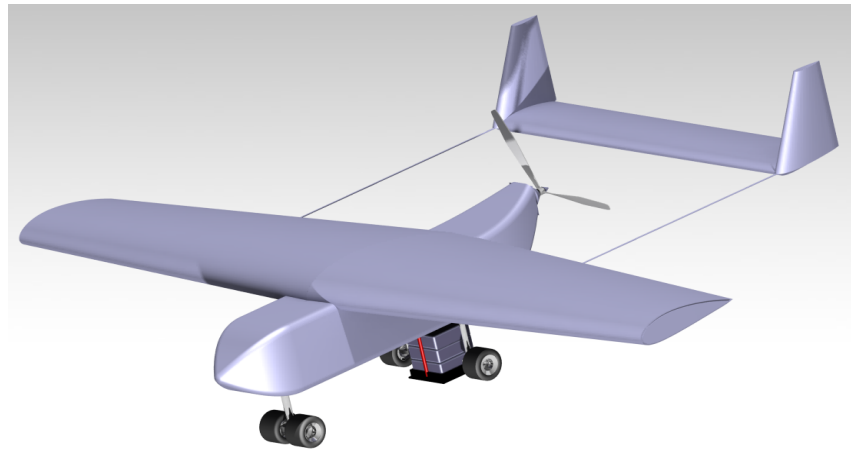


Figure 6: Concept2: Oblique view show salient features

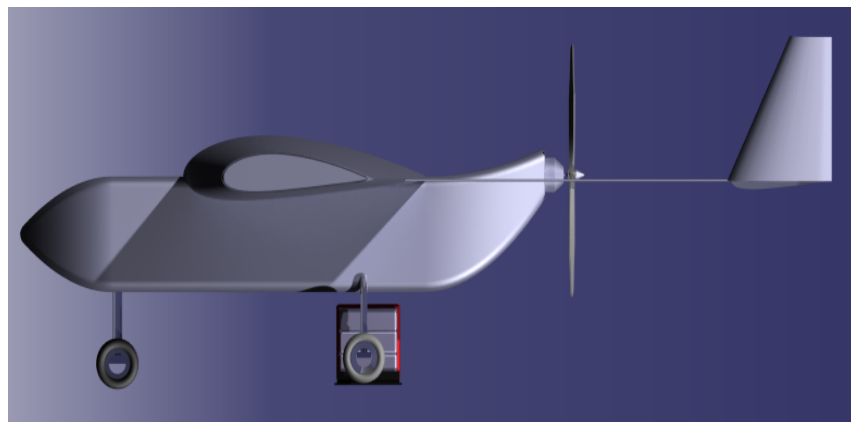


Figure 7: Concept2: Side view

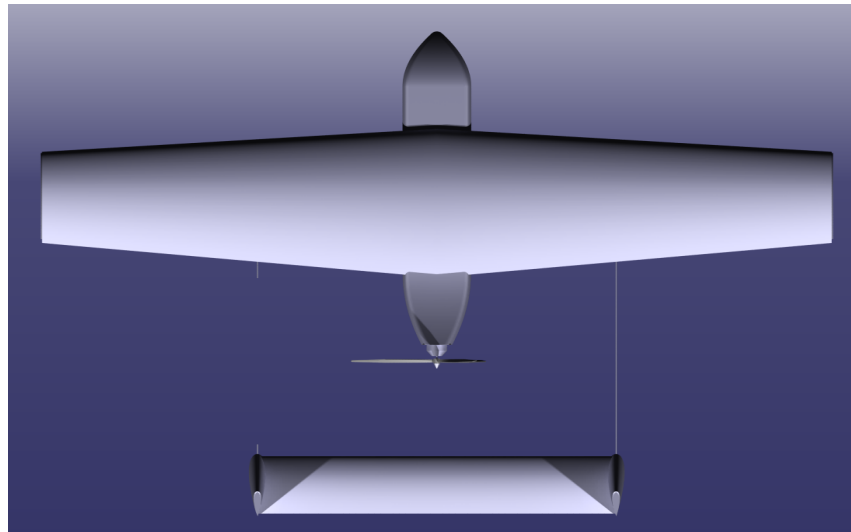


Figure 8: Concept2: Top view with fuselage profile

4.1.3 Saurav Lal Srivastwa (sausr199) Concept 3:

The design concept is inspired by commercial RC aircraft available in the market and meets every design parameter proposed by SAE Brazil. The aircraft has a rectangular-mid wing configuration with a 0.4m chord length and a 2m wingspan. According to the instruction manual provided by SAE Brazil, the sum of the total height and wing span should not exceed 2.9 m and this design comes well within the limits.

WING AND TAIL CONFIGURATION:

Rectangular wings stalls at the wing root. This makes the wing incredibly maneuverable because the stall starts at the wing base, reaching the control surfaces (ailerons and flaps) last. Mid-wing configuration was chosen here because the overall drags tend to be lower. On the other hand, the H-tail configuration allows the positioning of the vertical tails in undisturbed air during high-angle-of-attack conditions which thereby allows the aircraft to fly at lower speeds without stalling. The reason for two vertical stabilizers is to enable the aircraft to be highly maneuverable which is challenging for a single vertical tail aircraft in a high angle of attack situation. [6]

FUSELAGE:

Rectangular fuselage with dimensions $0.2 \times 1.42 \times 0.2$ m was simply chosen due to ease of construction. The fuselage also partially houses the payload of 5kg inside the body with a slight extension outwards as shown in Fig. 10.

PAYOUTLOAD:

Lead was chosen as payload due to its high volume and the payload is placed just below the wing to balance the C.O.G.

LANDING GEAR:

Tricycle-fixed landing gear configuration is used to reduce the possibility of a ground loop as the main landing gear lies behind the C.O.G. It is also worth mentioning that this landing gear configuration is less vulnerable to cross winds making the aircraft stable in the air, Fig. 9 and Fig. 10 respectively give a 2-D and 3-D view of the aircraft landing gear.

MOTOR MOUNTING AND PROPELLERS:

The aircraft gets its propulsion from a front-mounted electric motor with a 2-blade propeller of length 0.4 m. This provides better control over the pitch and yaw and leads to improved balance and stability. Fig. 9 and Fig. 10 respectively give a 2-D and 3-D Isometric view of the motor and propeller mounting.

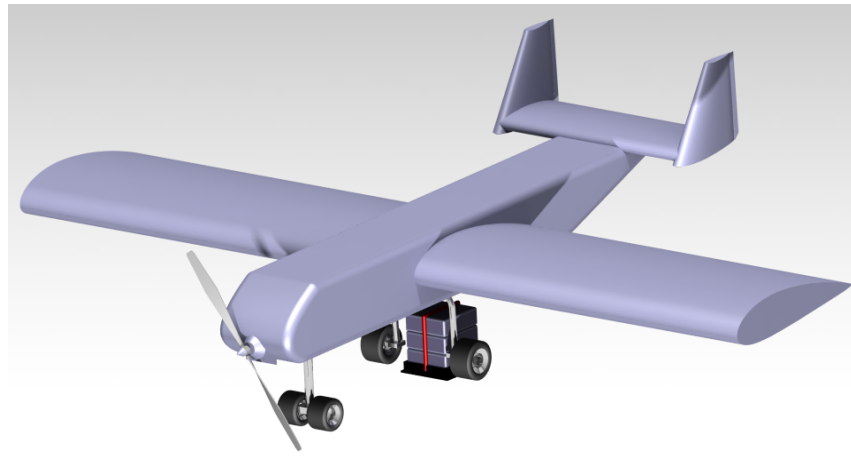


Figure 9: Concept3: Oblique view show salient features

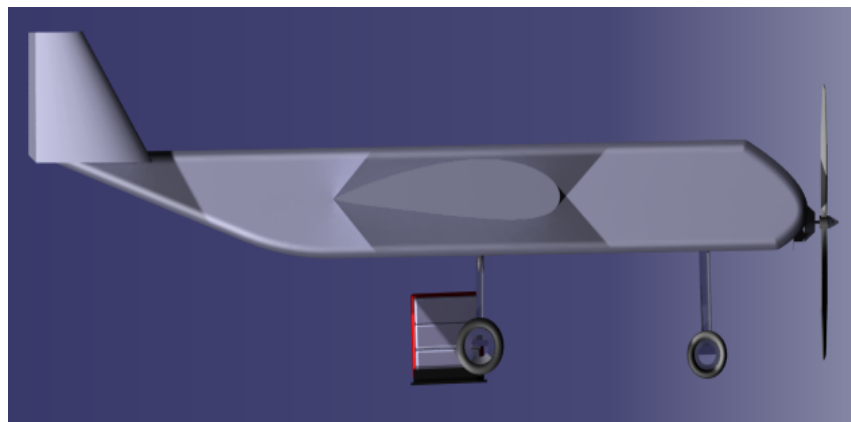


Figure 10: Concept3: Side view

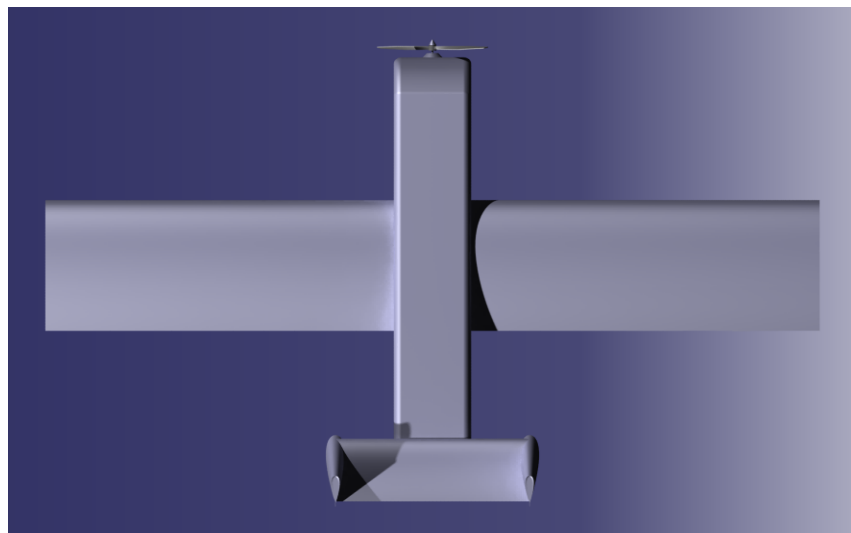


Figure 11: Concept3: Top view with fuselage profile

4.1.4 Aditya Mohan Jaiswal (adija250) Concept 4: & Abhishek Dhiman (abhdh352) Concept 5:

The two design concepts proposed by Aditya (Concept 4) and Abhishek (Concept 5) were almost similar giving them a high commonality index and fitting the RCAs well within the design requirements of SAE AeroDesign Brazil, 2023. **The distinguishing factor is the choice of wing planform trapezoidal for Concept 4 (Aditya) and rectangular for Concept 5 (Abhishek).** The two designs are discussed below.

Wing & Horizontal Configuration:

Selecting the wing plan form is fundamental for aerodynamic performance. The best would have been to choose an elliptical wing for uniform lift generation span-wise. But, considering the competition timelines, manufacturing complexities of elliptical planform, and expenses the idea is dropped for both concept 4 and concept 5.

1. Concept 4 (Aditya): The trapezoidal wing is mid-way between an elliptical and rectangular wing, enjoying the benefits of both planforms, hence selected for concept 4 for wing and horizontal stabilizer. The trapezoidal wing gives less surface and weight leading to lesser total drag and better lift distribution compared to the rectangular wing. But the wing tip is more prone to stall at high α leading to instability and control loss [6], [7], Fig. 12 and 14.

2. Concept 5 (Abhishek): The rectangular wing is selected for Concept 5. This planform for both wing and horizontal stabilizers gives high stability at low speeds, prone to wing root stalls hence maintaining stability at high α , and most importantly it is easy to manufacture, takes less time, and can be highly strengthened [6], [8]. With a demerit of no lift generation at the wing tips, Fig. 15.

The **fuselage, payload, empennage, landing gear, and nose-mounted propeller** are the same for concepts 4 and 5. The fuselage cross-section is opted to be square with dimensions of ($1.5 \times 0.18 \times 0.18 [m^3]$) to accommodate payload and extended payload (Lead [Pb]) blocks directly under the wing quarter chord (CG), Fig. 13 and 16. The landing gear has a pair of two wheels both before and after CG location to support the total weight during landing and distribute the impact evenly, Fig. 13 and 16. The nose-mounted propeller is selected to be 18-20 [inch] i.e ($0.4572 - 0.508$) [m] in diameter with twin blades to generate sufficient thrust for the MTOW with better pitch stability (aiding the pitch down moment), Fig. 12 and 15. The empennage is opted to be conventional which provides adequate stability and control with the least weight. It puts the horizontal tail in the smooth flow position most of the time [6].



Figure 12: Concept4: Oblique view show salient features

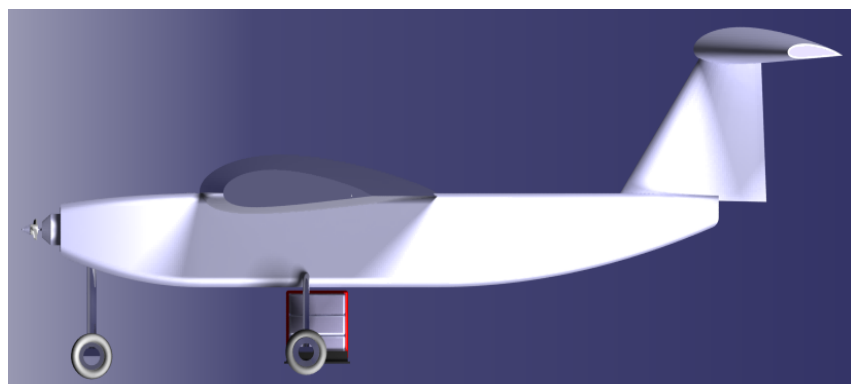


Figure 13: Concept4: Side view

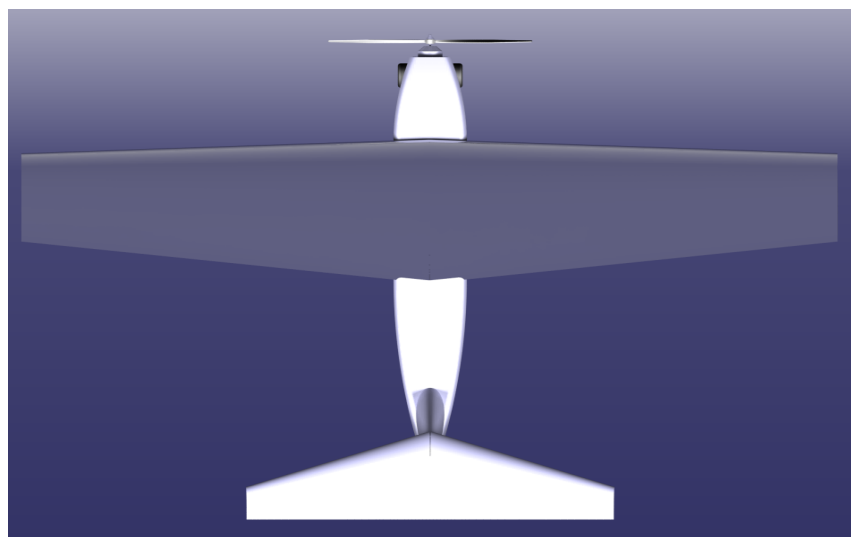


Figure 14: Concept4: Top view with fuselage profile



Figure 15: Concept5: Oblique view show salient features

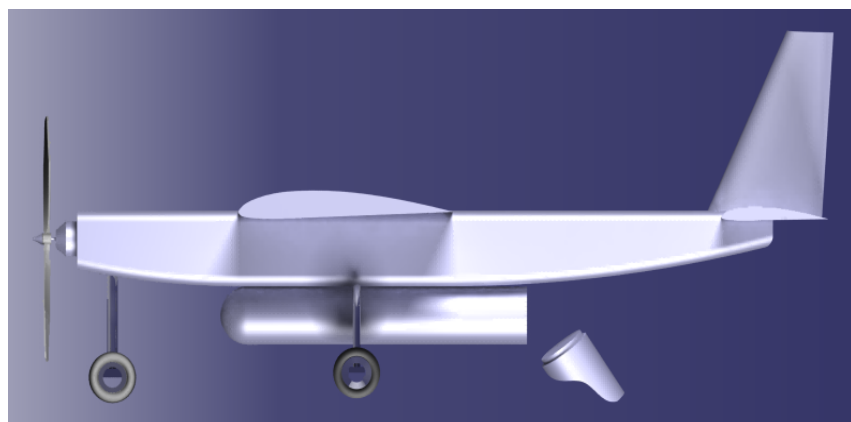


Figure 16: Concept5: Side view

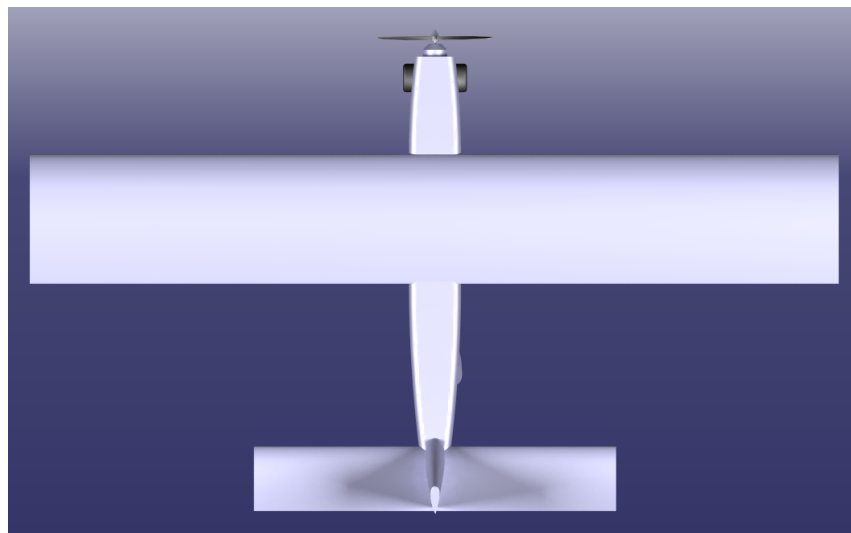


Figure 17: Concept5: Top view with fuselage profile

4.2 Concept Selection Process (MS3)

In the previous milestones, individual design concepts were introduced. In **MS-3**, the focus shifts towards concept selection. Out of the 5 design concepts, the final designs were chosen to be **tarna588's** and **concept6** concepts. Additionally, a new design concept was added based on feedback from Professor David Lundstrom. To summarize the selection process, a scoring matrix was generated as per SAE guidelines, which can be seen in Fig. 18.

The design selection matrix, also known as the generic selection matrix, is a method used to prioritize the best-optimized design by judging diverse options. Initially, a list of weighted criteria is formulated, and each design choice is assessed with certain criteria. The options are listed as rows in the table, and design choices are depicted as columns.

Certain selection criteria, such as lift and drag, hold more significance than others and are given higher weight-age. Fig. 18 shows all the significant selection criteria in the form of a matrix, denoted by H-high, M-medium, and L-low.

In **Step:1** of the concept selection process, the design evaluation points are identified. This is followed by **Step:2**, where the concept evaluation matrix is established to make objective decisions without any subjectivity. The list of design choices is included as column headings.

Next, in **Step:3**, each evaluation factor is given an importance number (High=3, Medium =2, Low=1), which is multiplied by the given score for each concept. This helps to improve the weight of the concept features.

Finally, in **Step:5**, the weighted scores for each concept are added to arrive at the ultimate scores.

Parameters	Size	Lift	Drag	OEW	Production Cost	Prodction Ease	Payload	Stability	Safety	Portability	Total_Score (High better)
Importance	3	3	3	2	2	2	3	2	3	1	
DP1 (yeshwanth)	3	6	3	2	6	6	6	4	9	3	48
DP2 (tarun)	9	9	6	4	2	4	6	4	6	1	51
DP3 (saurav)	3	3	6	2	2	2	6	6	6	3	39
DP4 (aditya)	6	9	3	2	4	4	6	6	9	2	51
DP5 (abhishek)	6	6	6	4	6	4	9	4	9	3	57
DP6 (Integrated design)	9	9	9	6	4	2	9	6	9	3	66
					Scoring			Importance			
					1	Poor		H	high	3	
					2	Average		M	medium	2	
					3	Good		L	low	1	

Figure 18: Scoring Matrix Of Concept Selection Process

4.3 Individual Concepts Convergence

After some brainstorming regarding the payload and better aerodynamic efficiency of the aircraft, the team proposed to integrate the designs of each team member. The idea was to eliminate the cons of each of the concepts while maintaining the merits of each of the concepts. Another major aspect was to reduce the fuselage volume which will thereby reduce the total drag. The payload-carrying compartment was the main focus, since the higher the payload higher the points achieved in the competition. Thus keeping all the constraints in mind and aiming to implement them in the best way possible, the decision was made to go forward with the two designs as seen in Fig. 19 and Fig. 20. **Note that one of the designs has a variable payload compartment which can be attached above or below the fuselage (as seen in Fig. 21 thereby allowing fast removal of the payload leading to bonus points.**

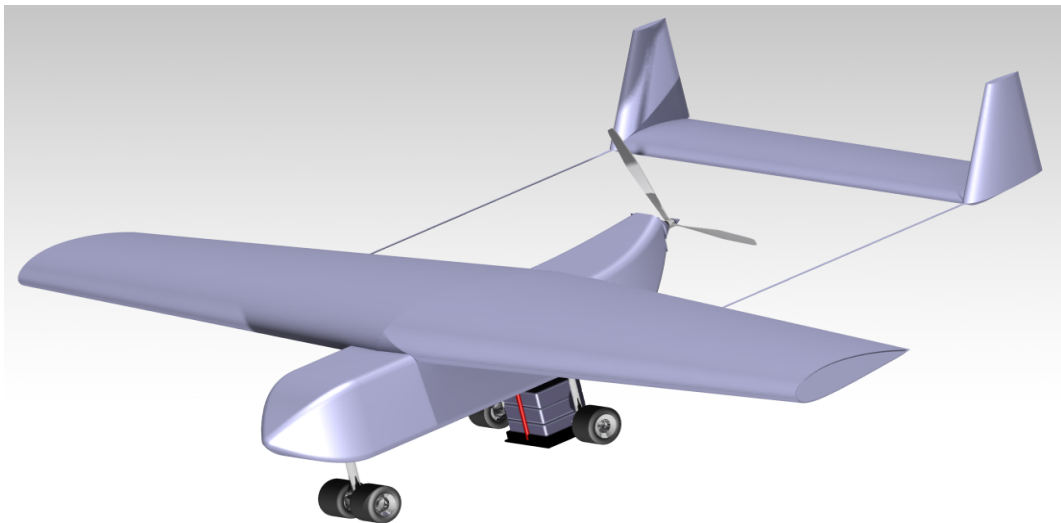


Figure 19: Concept2: Oblique View

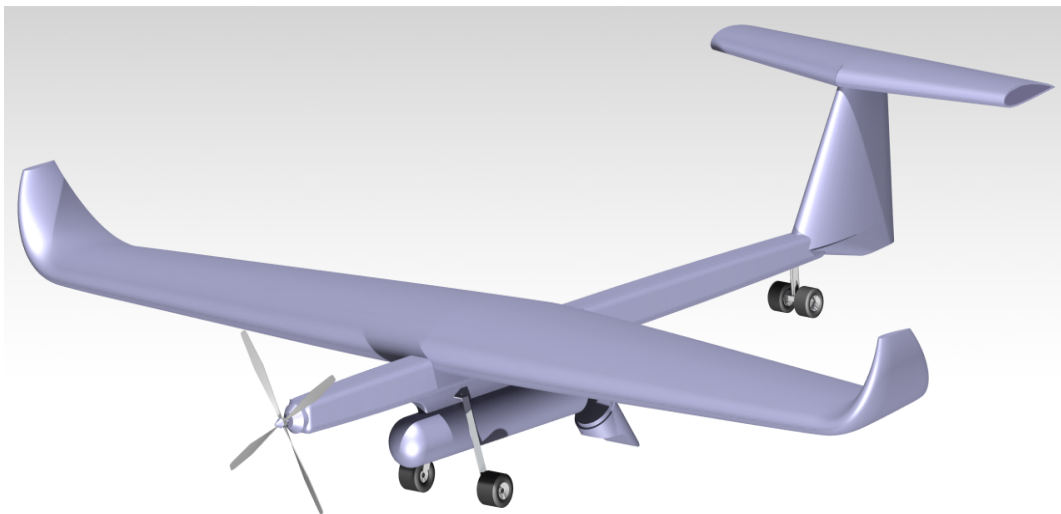


Figure 20: Concept6: Work in progress

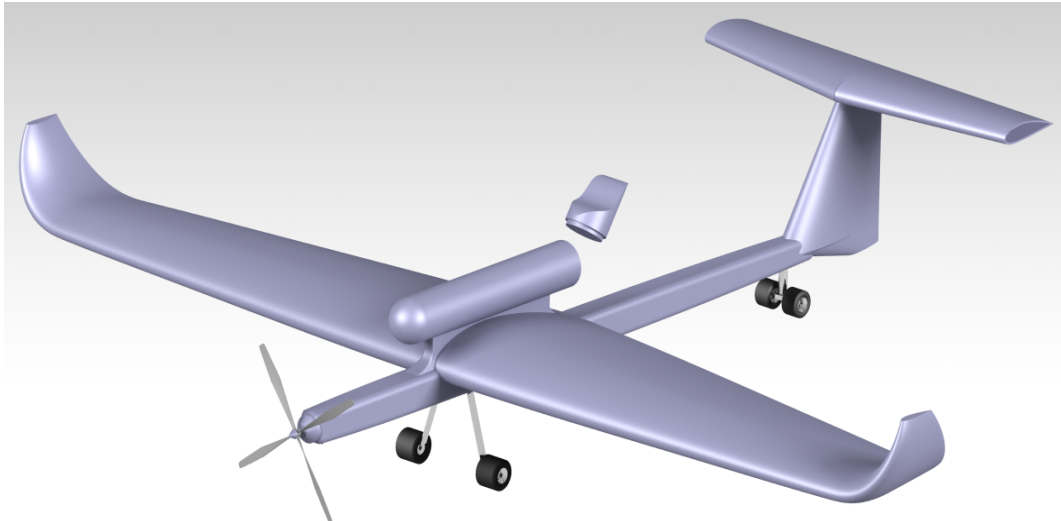


Figure 21: Concept6:Work in progress with variable payload placement

The idea behind keeping variable payload placement was to make the design flexible enough to carry heavy payload while maintaining its stability and aerodynamic efficiency. It can also be noted that this design can freely choose between a tail-dragger or tricycle landing gear configuration. This also gives the freedom of having a smaller or larger landing gear thus providing better ground clearance, as well as different propeller lengths if needed. Further study is required in order to understand the landing gear placement and the effects of the payload compartment on the aircraft's performance in context with structural strength, but for now, this design gives a much-needed advantage over all the other design concepts.

4.4 Final CAD Design (MS4)

In order to proceed with the course as well as with high hopes of designing an aircraft that could win the SAE competition, two final designs were selected. These two designs can be seen in Fig. 22 and 25. The first design is a merger between the two concepts selected in the previous milestone, taking the pros of each concept while eliminating the cons as much as possible. It could be noted that having the payload below the fuselage, the aircraft needed to have a bigger landing gear which in turn increased the maximum height of the aircraft. Since according to the rules of the competition the maximum height of the aircraft should not exceed 0.6 [m], a H-tail configuration was chosen in order to have smaller vertical stabilizers, thereby reducing the overall aircraft height while having better yaw control with the help of two vertical stabilizers. The H tail also allows the aircraft to fly slower without stalling which is an added benefit for the aircraft. The top and side view can be seen in Fig. 23 and 24.

The team came up with a better and optimized version of the aircraft, with a better payload placement while trying to keep the maximum height of the aircraft in check. The final result of this optimization led to a new design as seen in Fig. 25. Though the design has some manufacturing complications, the overall pros exceed the cons by a margin. The payload compartment was removed altogether as the fuselage and wing combined are used as the payload compartment. The payload comprises of multiple steel rings which are connected together with the help of a road and stoppers to stop their movement during flight. The wing is connected with the help of two central spars, and most of the payload is kept within the center of the two spars, thereby almost on top of the CG of the aircraft. In order to achieve extra points in the competition, extra payload(in equal mass) can be added ahead of the first spar and behind the second spar, thereby maintaining the CG of the aircraft. This payload configuration allows us to reduce the overall empty weight of the aircraft as there is no need to include a payload compartment, as seen in Fig. 36. The aircraft uses a T-tail configuration which not only provides the aircraft with glide characteristics(needed for better landing with heavy payload) but also provides better low-speed stability by reducing induced drag. The elevator being above most of the downwash from the propeller and wing is again an added benefit. The top and side view can be seen in Fig. 26 and 27. Both the designs use tri-cycle landing gear configuration as they not only reduce the possibility of ground loops but also are less vulnerable to crosswinds. Since the site where the competition takes place is usually windy, tri-cycle landing gear was the optimal choice for the aircraft.

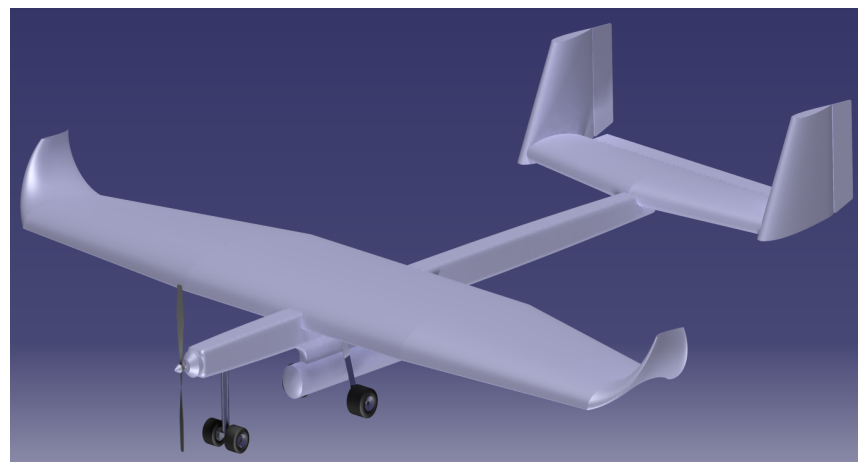


Figure 22: Isometric view for the first design

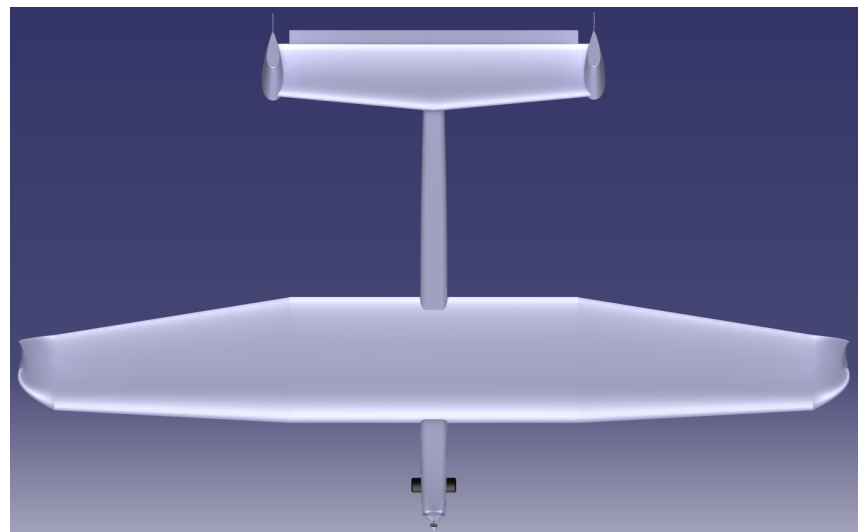


Figure 23: Top view for the first design

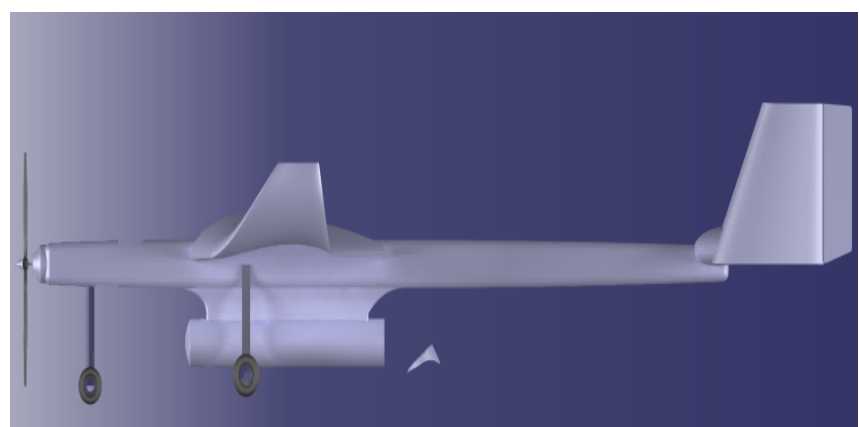


Figure 24: Side view for the first design



Figure 25: Isometric view for the second design

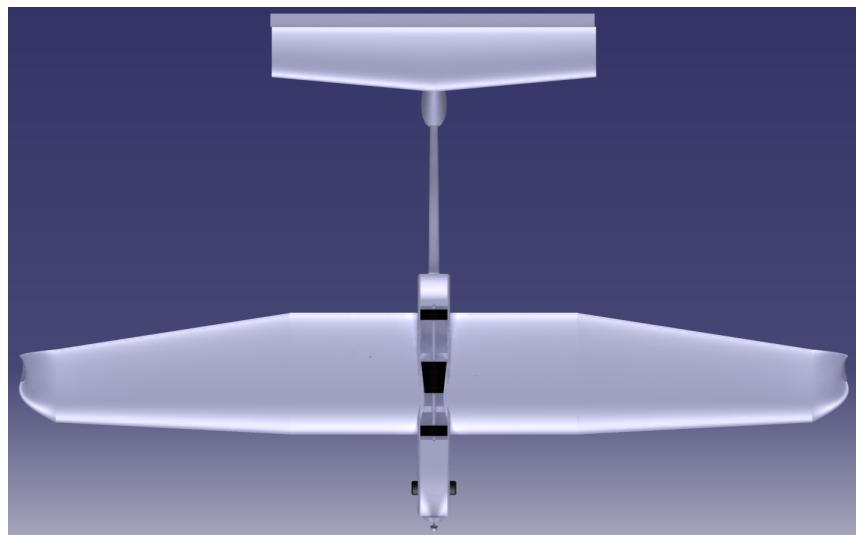


Figure 26: Top view for the second design

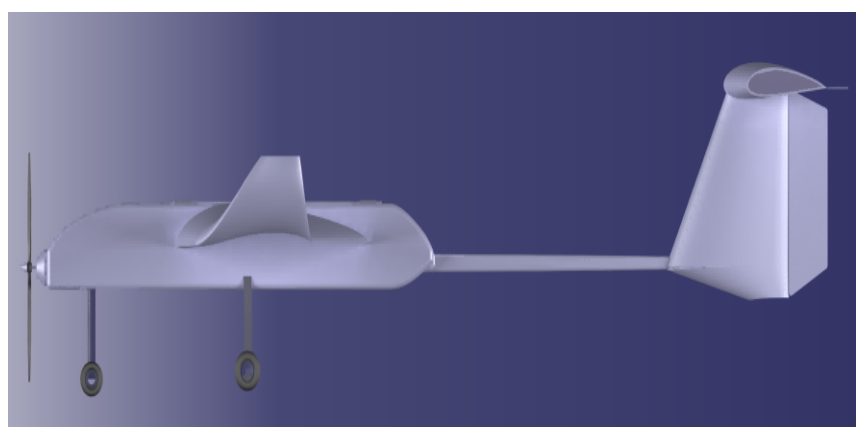


Figure 27: Side view for the second design

4.5 Finalized Concept: Detailed CAD Model

Further optimization and analysis led to the final design of the aircraft for the mission profile in the competition. The design takes into consideration the discussions in supervision sessions, fellow students and almost all the merits of the previous designs while trying to eliminate as many demerits as possible. One of the major aspects of an aircraft is its wing design, which was significantly changed to produce higher lift and better lift distribution over complete span of the wing. Another important change was to invert the horizontal tail, in order to produce negative lift during flight to make the aircraft stable and counteract upward pitching moment from the horizontal tail. The detailed CAD model with different views can be seen from the Fig. 28 to 34. The internal sections for the electrical components such as the battery and ESC, along with the payload compartment can be seen in the Fig. 35. The payload will be partially shared by the fuselage and wing, while being separated by the spars, which will be connecting the wing with fuselage. The minimum required payload (5 kg) will be placed between the two spars, while extra payload reaching up to 10 [kg] will be placed in equal amounts in front of the leading spar and behind the trailing spar, thereby maintaining the overall CG of the aircraft. The payload placement can be seen in the Fig. 36. In order to share the weight of the the payload additional supports will be added which will sit on the fuselage, which can be seen in Fig. 37. Furthermore the servo locations for the control surfaces can be seen in the Fig. 38 to 40 in form of black markers. The detailed draft of the aircraft with important dimensions of the aircraft can be seen in the Fig. 41. It can be noted that the ground reference line only offers an angle of $5^\circ - 6^\circ$. Although this would be an issue for a normal aircraft but since this aircraft has a good incidence angle for the wing by default along with ample distance for take off, the aircraft should be able to take off with ease without requiring high pitch angles.

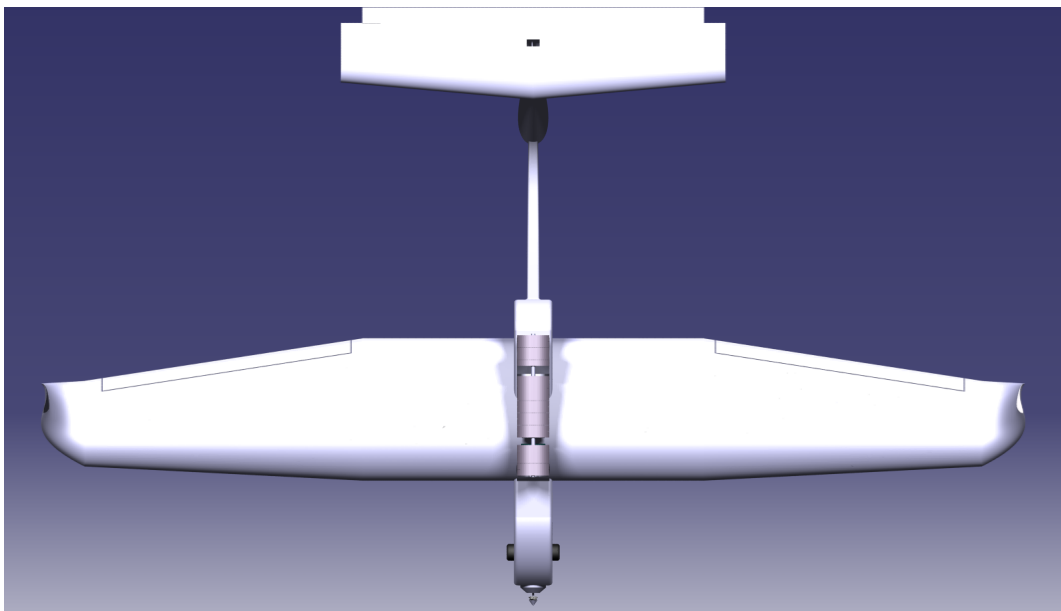


Figure 28: Top view of the finalized model

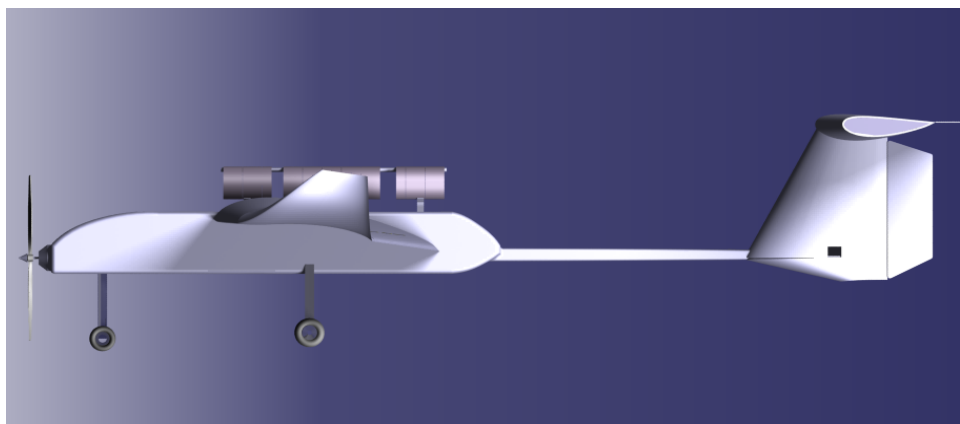


Figure 29: Side view of the finalized model

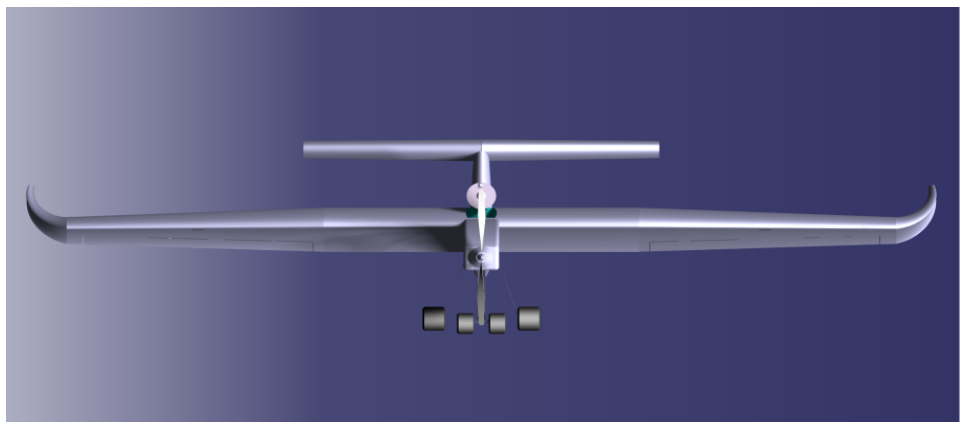


Figure 30: Front view of the finalized model

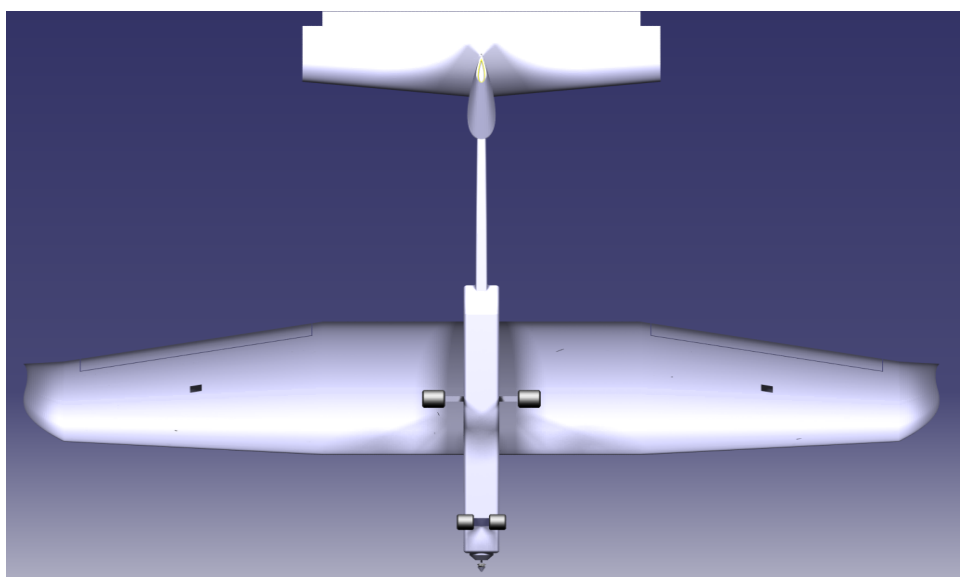


Figure 31: Bottom view of the finalized model

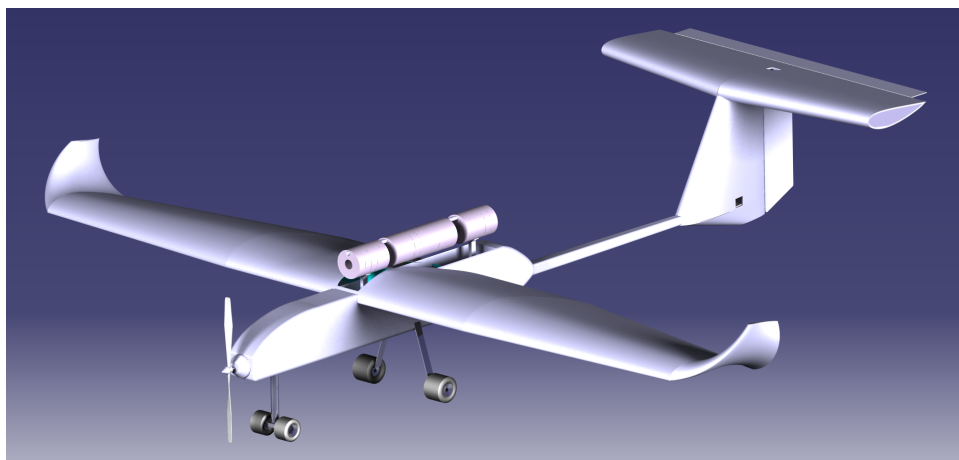


Figure 32: Isometric view of the finalized model with full payload 10 [kg]

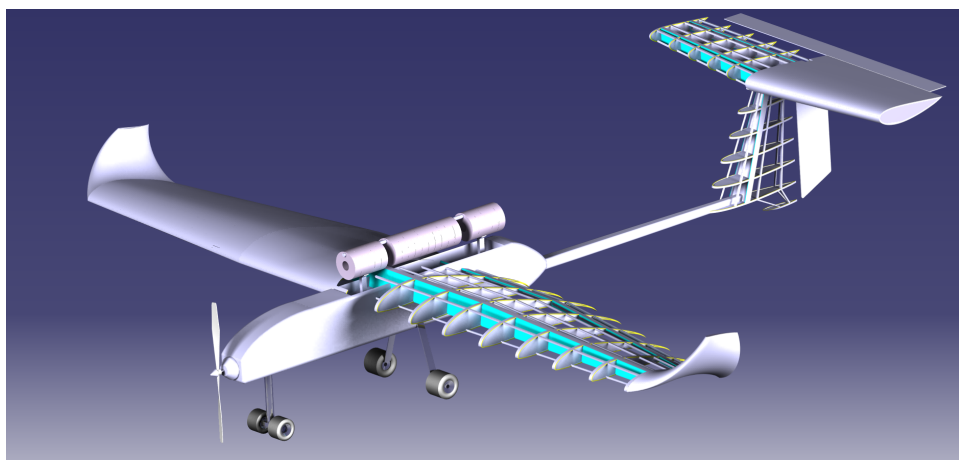


Figure 33: Internal structure of the finalized model wing and tail

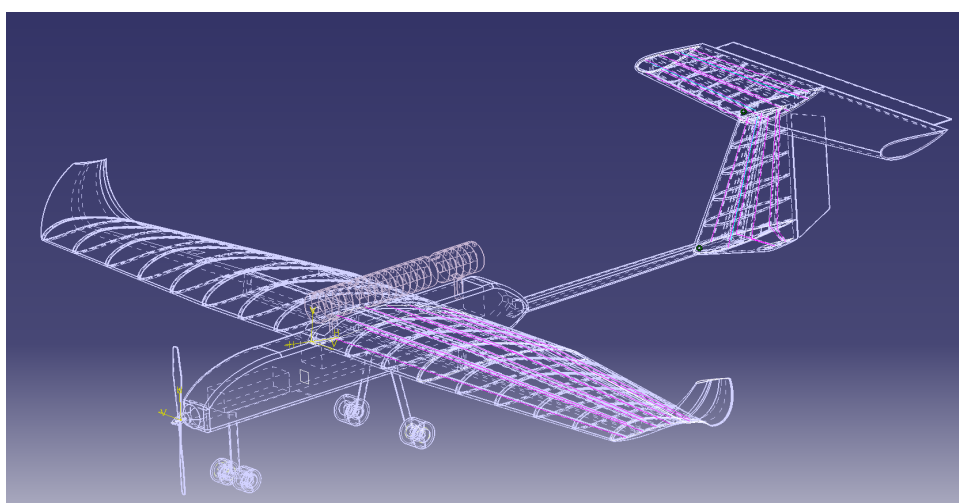


Figure 34: Skeletal structure of the finalized model

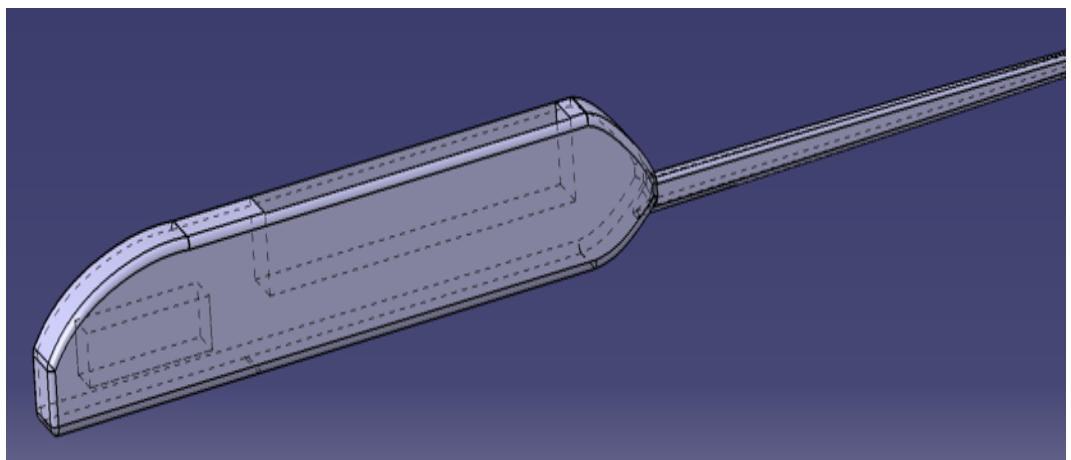


Figure 35: Internal section for the electric components and the payload

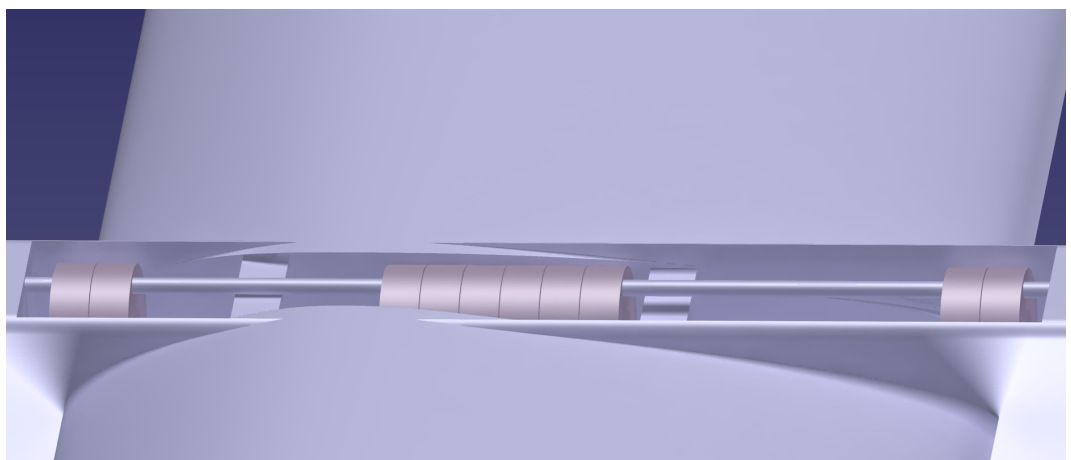


Figure 36: Payload comprising of stainless steel plates, weight range [5-10] kg

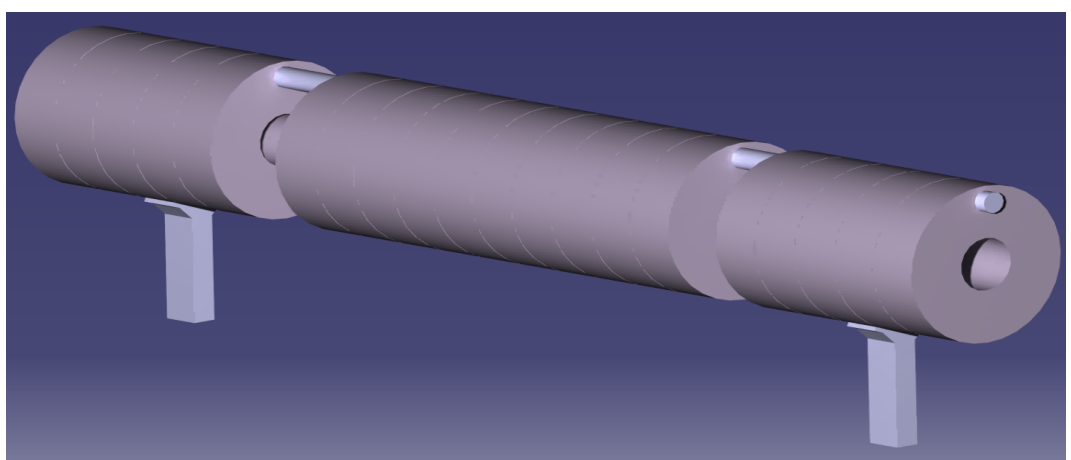


Figure 37: Payload comprising of stainless steel plates, weight range [5-10] kg

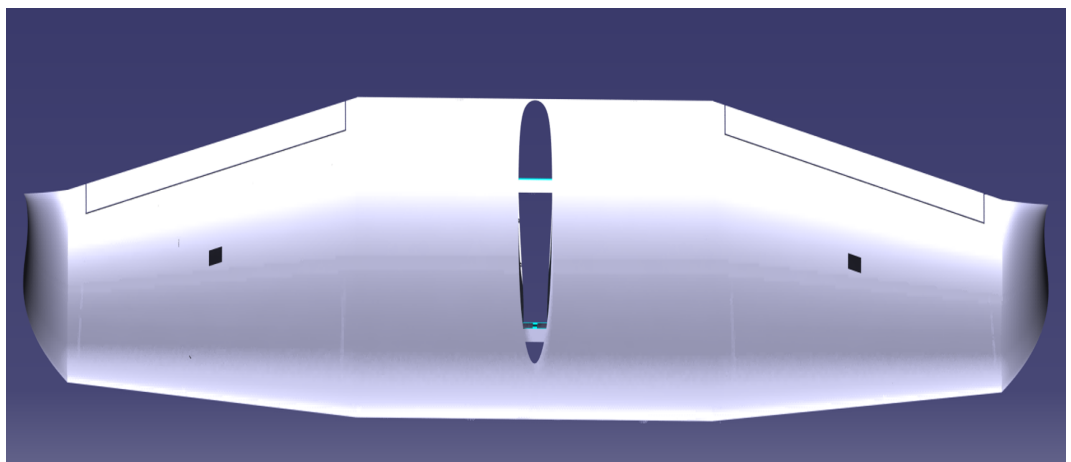


Figure 38: Servo locations on the wing for ailerons

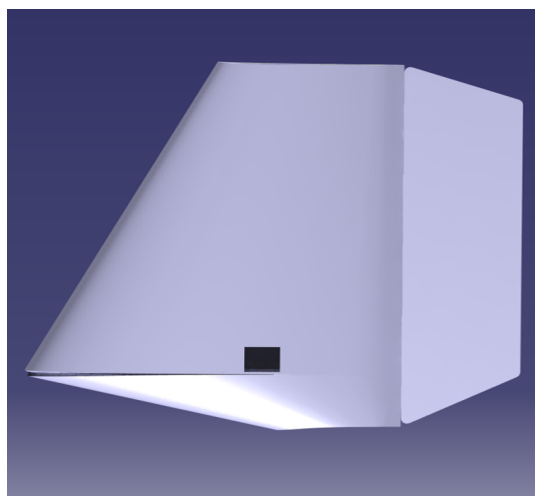


Figure 39: Servo locations on the vertical tail for rudder

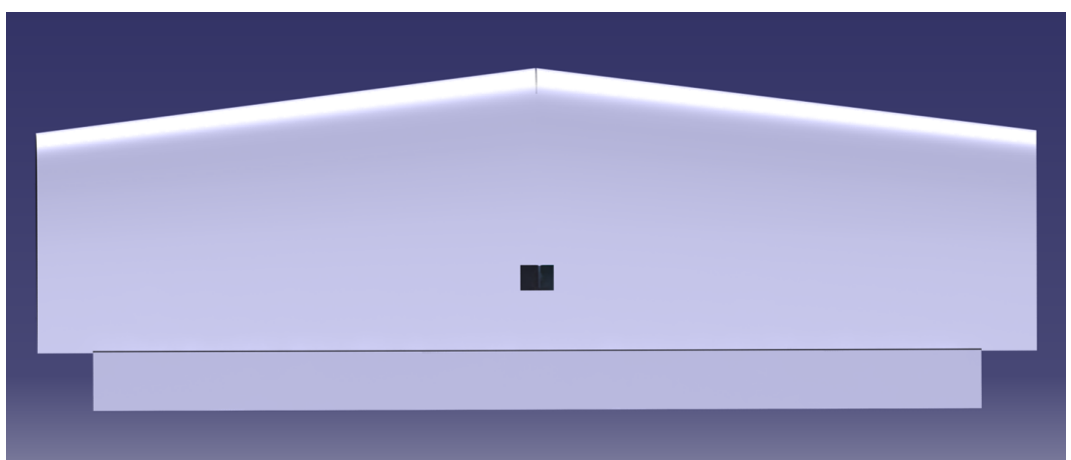


Figure 40: Servo locations on the horizontal tail for elevator

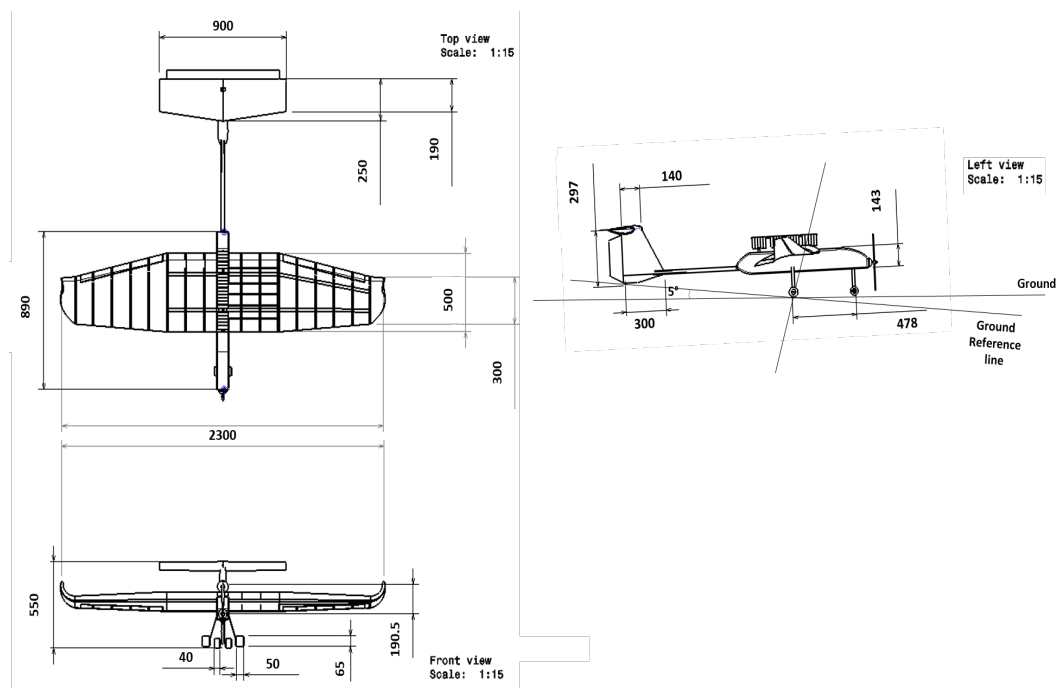


Figure 41: Finalized draft of the model with specific dimensions

4.6 Final Design Sizing Diagram

$$\frac{T}{W} = \frac{1.21}{g\rho C_{L_{max}} \cdot S_G} * \frac{W}{S} + \frac{0.605}{C_{L_{max}}} * (C_{D_{TO}} - \mu C_{LTO}) + \mu [2] \quad (1)$$

$$\frac{T}{W} = \frac{V_v}{V_\infty} + \frac{q}{W/S} C_{D_{min}} + \frac{k}{q} \cdot \left(\frac{W}{S}\right) [2] \quad (2)$$

$$\frac{T}{W} = \sin \gamma + \frac{1}{LD_{max}} = \sin \gamma + \sqrt{4K C_{D_{min}}} [2] \quad (3)$$

$$\frac{T}{W} = q * \left[\frac{C_{D_{min}}}{(W/S)} + K(n/q)^2 \left(\frac{W}{S}\right) \right] [2] \quad (4)$$

$$\frac{T}{W} = q * \left[\frac{C_{D_{min}}}{(W/S)} + K(n/q)^2 \left(\frac{W}{S}\right) \right] + \frac{P_S}{V_\infty} [2] \quad (5)$$

$$S_{L_{DSG}} = 19.08 h_{obst} + [0.008 + 1.556\tau \sqrt{\frac{A}{W/S}} + \frac{1.21}{g[\frac{0.605}{C_{L_{max}}}(C_{D_{LDG}} - \mu C_{L_{LDG}}) + \mu - \frac{T_{gr}}{W}]} \frac{W/S}{A}] [2] \quad (6)$$

where,

C_{LTO} = Lift coefficient during T-O run

C_{DTO} = Drag coefficient during T-O run

ρ = Density at sea level

$C_{L_{max}}$ = Maximum lift coefficient T-O configuration

S_G = Ground run (ft or m)

μ = Ground friction constant (typ.0.04)

g = Acceleration due to gravity (ft/s² or m/s²)

q = Dynamic pressure at the selected airspeed and altitude (lb_f/ft² or N/m²)

V_∞ = Airspeed (ft/s or m/s) typically v_γ

V_v = Vertical speed (ft/s or m/s²)

LD_{max} = Expected maximum L/D

γ = Desired climb angle

C_{Dmin} = Minimum drag co-efficient

k = Lift-induced drag constant

$n = \text{Load factor} = \frac{1}{\cos \phi}$

P_S = Specific excess power at the condition

h_{obst} = Obstacle height(typ.50 ft for GA, 35 ft for commercial)

$A = \rho C_{L_{max}} (\text{ in slugs/ ft}^3 \text{ of kg/m}^3)$

$C_{L_{LDG}}$ = Lift coefficient in the ground roll

$C_{D_{LDG}}$ = Drag coefficient in the ground roll

τ = Time for a free roll before braking begins (typ.1-5s)

$\frac{T_{gr}}{W}$ = Thrust loading during the ground roll, where T is idle or reverse thrust.

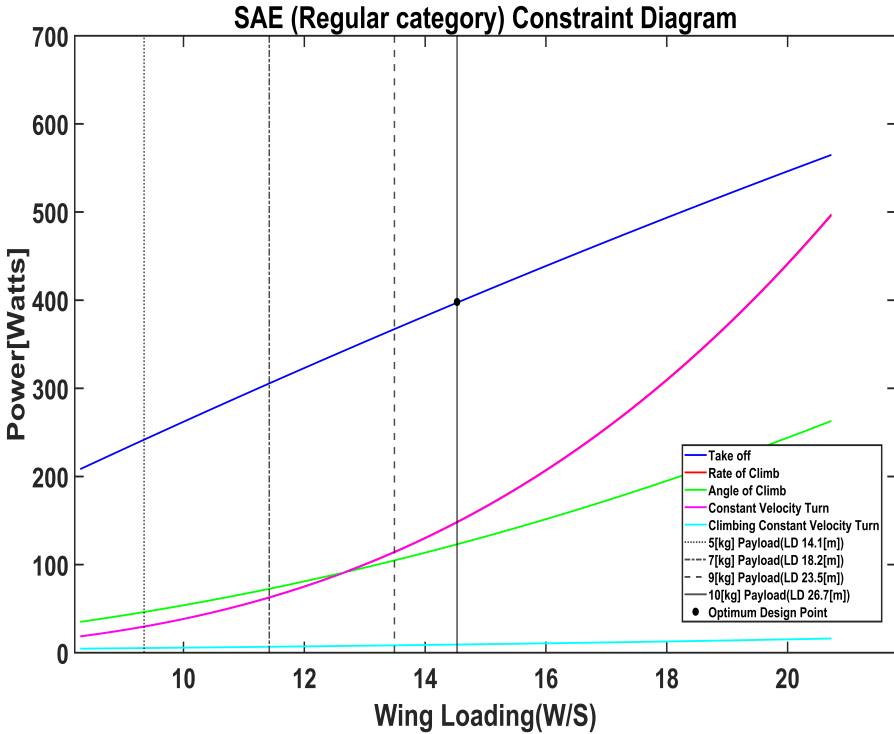


Figure 42: Constraint Diagram

When designing an aircraft that utilizes a Propeller motor, creating a Constraint Diagram is an essential step to determine the aircraft's Wing-Loading (W/S) and Power (P). The graphical representation in this case is constrained by the Power-Loading (P/W) formula. In order to solve the necessary equations, various variables such as Airspeed (V), Ground Friction Coefficient (μ) is inputted into MATLAB and the corresponding Lift, Drag, $C_{l,max}$ are found out using a atmosphere code for the Density (ρ) with changes in altitude, velocities and the Component build-up method is used for the drag and lift calculations for the varying densities and velocities these values are inputted into The Take-Off variable is the first factor represented in the constraint diagram using Equation [1], as shown in Fig. 42. The SAE constraint diagram is constructed using Equations [2], [3], [4], and [5].

The obtained Thrust to weight ratios are converted to Power by multiplying with velocity and Weights to check the power required at the corresponding wing loading of the required MTOW and the optimum design point obtained was taken at the $14.9(kg/m^3)$. This optimum design point was selected based on the landing distance Section. 6.1 and Wing-loading required for a 10 [kg] payload. Form the constraint diagram it was observed that aircraft needs 400-500 [W] for it to carry 10 [kg] payload and a 4.1 [kg] of empty weight.

5 Aerodynamic Analysis

5.1 Airfoil Performance

The serious challenge during the manufacture of Aircraft is choosing the best airfoil in which Wing will produce a good characteristic behavior of Lift coefficients and better bending moment resistance helps in providing evident lift that can carry or sustain high payloads. The Airfoil selection commences by brainstorming about the qualities which the team acquires in an airfoil various airfoils are studied finally after brief research over various airfoils the most suitable and better airfoils are selected which have good thickness and camber that assist the airfoil in the high lift, Various airfoils have opted with the help of scoring table of each airfoil based on the characteristics of the airfoil can be seen in Table. 4

Airfoil Scoring Table

Airfoil	C_l	C_d	C_m	C_l/C_d	C_l vs C_d	Total
E243	3	2	3	3	3	14
S1223	3	2	3	3	3	14
NACA23015	1	3	1	1	2	8
NACA2212	1	3	1	1	2	8
FX63137	2	1	3	2	3	11
NACA4415	1	2	2	3	2	10

From this Table. 4 we can see that **E243** and **S1223** airfoils achieved the highest score. This scoring was obtained by plotting the Coefficient of Lift, Coefficient of Drag, and Coefficient of Moment of the airfoils at (-8 → 20) degrees Angle of Attacks (AoA) range and Reynolds number of $220e^3$, This specific Reynolds number is chosen since the velocity of the aircraft for the Reynolds number is around **8 [m/s]** which the velocity at which the aircraft is flown at. The C_l vs C_d and C_l/C_d graphs along with the Coefficient of Lift, Coefficient of Drag, and Coefficient of Moment can be seen in Fig. 44, 43.

From the graphs in Fig. 43 and 44, Airfoil S1223 had the best C_l , low C_d , and the best C_m values and also the C_l vs C_d graph showed that airfoil S1223 having lower drag for higher lift, we can see that the lift of airfoil is Angle of Attack independent. Hence Airfoil **S1223** was selected for this competition.

5.2 Drag Polar

In this study total drag analysis of a Remote control(RC) aircraft are investigated using Matlab. S1223 airfoil is used for wing design and it is opted from Scoring table can be seen in Table. 4 this airfoil had scored highest score over remaining selected airfoils. when the aircraft is moving into the air it is subjected to aerodynamic forces. The aerodynamic forces are lift, drag, and thrust forces.

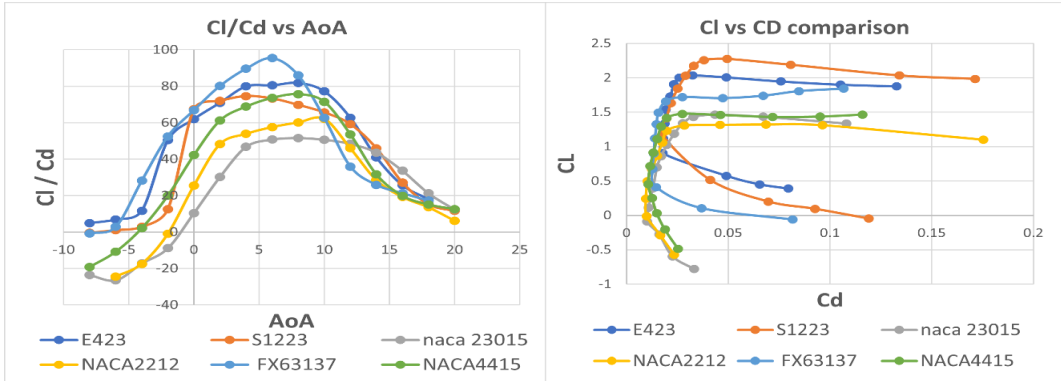


Figure 43: Cl/Cd and Cl vs Cd Graphs

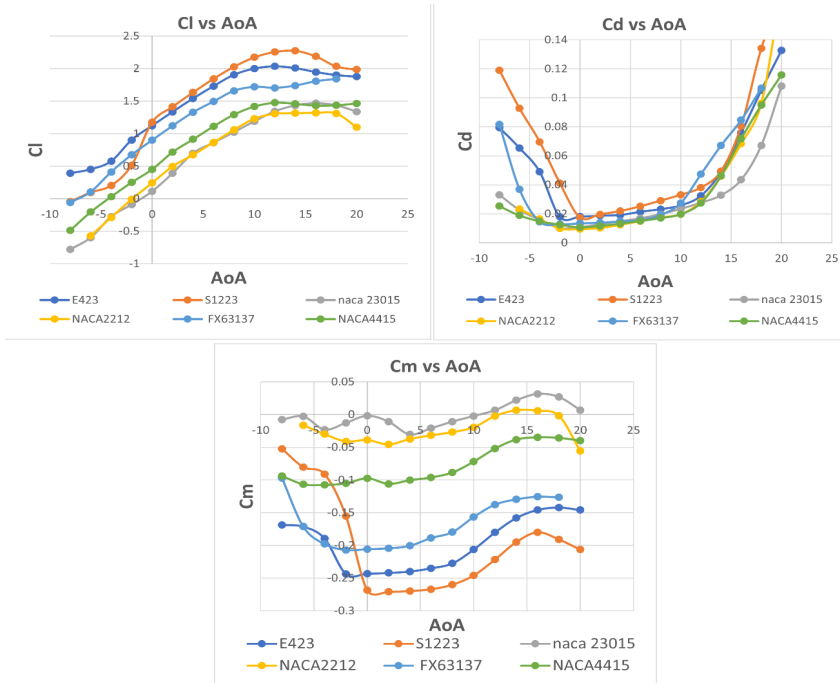


Figure 44: Airfoil Comparison Graphs

In aircraft design, the main objective is usually to minimize drag, to optimize it the methods to estimate drag of different parts of its causes and prevention. To model the drag of an aircraft it is a mathematical expression of the drag coefficient for a body, it describes mainly how the drag of the body changes with orientation in the flow field. A drag model is a mathematical representation of the drag coefficient of a body. It is denoted by C_d for 2D bodies and C_D for 3D bodies. The total drag of the aircraft are classified in to Zero-lift drag(parasite drag) and INDUCED DRAG . The major contributors to **Parasite drag**) are Pressure and Skin-friction drag. The pressure drag is generated by the pressure differential formed by the body and Skin friction drag is caused by the the particles are rubbing against the body surface. The parasite drag C_{D_O} is calculated by using component- build up method.

It means that the parasite drag C_{D_O} is computed for wing, horizontal tail, vertical tail, and fuselage individually by using Eq. 8 and adding 5% miscellaneous drag of individual components and in the parasite drag equation other parameters are required like skin friction coefficient, Form factor, Interference factor, and Wetted area for all components of aircraft these are calculated from using following Eq. 8-12. On the other hand **Induce Drag** was calculated from Eq. 15 in that Oswald efficiency factor is calculated from Eq. 17 then Finally the total drag is summation of both parasite drag and induced drag can be seen in Eq. 18 by using this Total drag(C_D) is computed

Parasite Drag:

$$C_{D_O} = C_{f_e} * \frac{S_{wet}}{S_{ref}} [6] \quad (7)$$

$$C_{D_0} = \frac{\sum (C_{fc} * FF_c * Q_c * S_{wet,c})}{S_{ref}} + C_{D_{misc}} + C_{D_{L\&P}} [6] \quad (8)$$

Equivalent Skin Friction coefficient

$$C_{f_e} = (C_{fc} * FF_c * Q_c) [6] \quad (9)$$

Flat plate Skin Friction Coefficient(turbulent):

$$C_{f,turb} = \frac{0.455}{(\log_{10}(Re))^{2.58}(1 + 0.144M^2)^{0.65}} [6] \quad (10)$$

Form Factor(FF) Wing and Tail

$$FF_{Wing,Tail} = \left[1 + \frac{0.6}{(x/c)_m} \left(\frac{t}{c} \right) + 100 \left(\frac{t}{c} \right)^4 \right] [1.34M^{0.18}(\cos\Lambda_m)^{0.28}] [6] \quad (11)$$

Fuselage:

$$FF_{Fuse} = \left(1 + \frac{5}{f^{1.5}} + \frac{f}{400} \right) [6] \quad (12)$$

Interference factor(Q)

$$Q_{wing} = 1$$

$$Q_{fuselage} = 1$$

$$Q_{Tail} = 1.06$$

Wetted Area: Wing,Tail:

$$S_{wet} = S_{exposed} \left[1.977 + 0.52 \left(\frac{t}{c} \right) \right] [6] \quad (13)$$

Fuselage:

$$S_{wet} = 3.4 * A_{side} [6] \quad (14)$$

Induced Drag:

$$C_{D_i} = \frac{C_L^2}{\pi \cdot AR \cdot e} = K \cdot C_L^2 [6] \quad (15)$$

$$K = \frac{1}{\pi \cdot AR \cdot e} [6] \quad (16)$$

For No sweep

$$e = 1.78 \cdot (1 - 0.045 \cdot A^{0.68}) - 0.64 [6] \quad (17)$$

Total Drag

$$C_D = C_{D_o} + C_{D_i} [6] \quad (18)$$

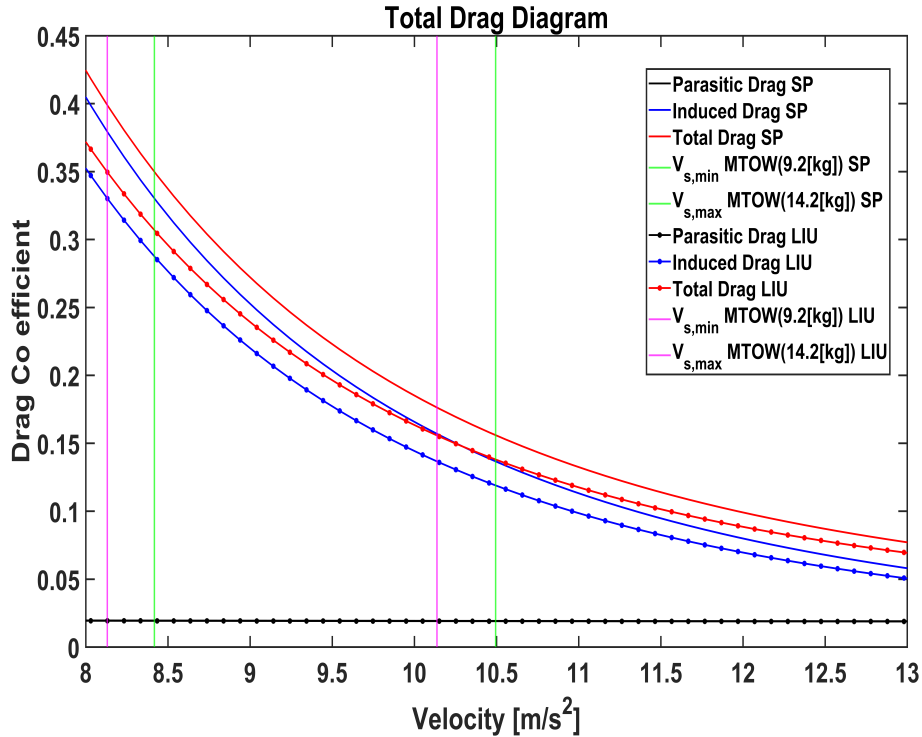


Figure 45: Total Drag graph

The variation of drag force as a function of airspeed velocity looks like a graph of parabola can be seen in Fig. 45 the consideration of separate sources of drag contribute total drag of an aircraft. From the graph it indicates that the drag reduces with velocity and got stabilized as increment of velocity. It specifies that there are some parameters will decrease the drag as the velocity increases. The comparison of parasite and induced drag is plotted in both Linkoping (LIU) and São Paulo (SP) regions based on density variations. This observation shown us the Induced drag (C_{D_i}) is higher in São Paulo (SP) compared to Linkoping (LIU) because the elevation is more in São Paulo (SP). On the other hand the Parasite drag (C_{D_o}) is same on both the regions so these confirms the total drag is high on São Paulo (SP) compared to Linkoping (LIU) which says that the additional lift is required in the SAE competition. There are vertical lines in Fig. 45 represents the Stall speed ($V_{s,max}$, $V_{s,min}$) of different MTOW weights at minimum and maximum speeds.

The stall speed is more in São Paulo (SP) due to more Total drag (C_D). The induced drag is reducing as velocity increases because the (C_{D_i}) is inversely as function of velocity.

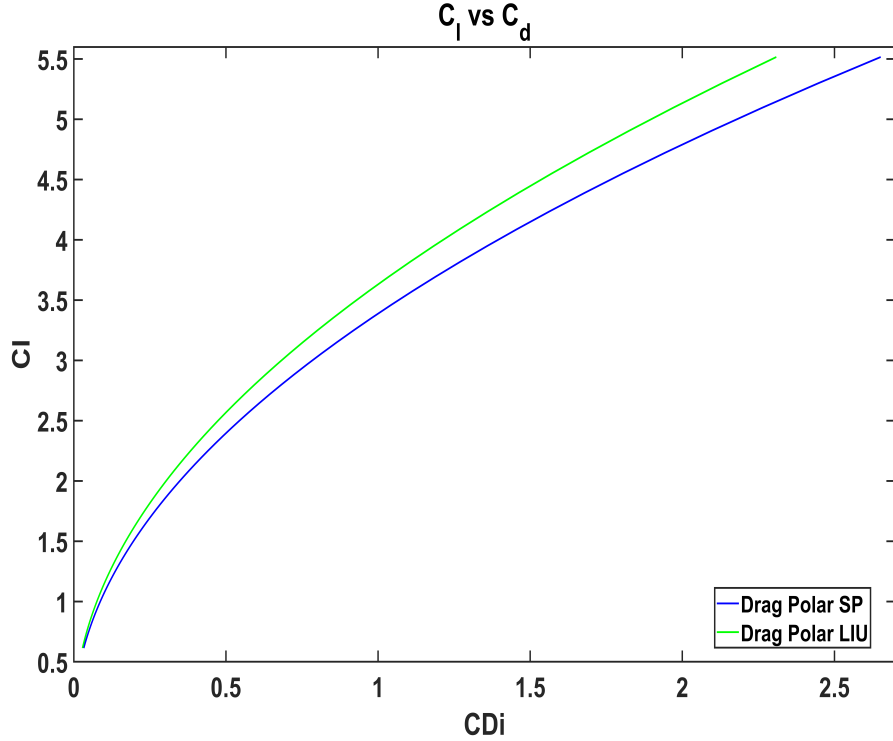


Figure 46: Drag Polar

In Fig. 46 the Drag polar is plot as the drag coefficient (C_d) function of lift coefficient (C_l) the parabolic drag has been selected at both Linkoping (LIU) and São Paulo (SP) regions. Note this curve starts from the stall speed, since the aircraft is not able to maintain the sustain level flight below the stall speed so due to the more Induced drag (C_{D_i}) in São Paulo (SP) from the previous diagram the requirement of lift coefficient (C_l) needs more, but it is small. The lift coefficient (C_l) is high due to density variations in Linkoping (LIU). The drag can be calculated accurately using mathematical second order parabolic curve.

6 Performance Analysis

6.1 Takeoff (TO) and Landing (LD)

6.1.1 Takeoff (TO)

The TO maneuver consists of several segments as illustrated in Fig. 47. The **Ground run** refers to the distance covered from brake release to the initiation of rotation, where the aircraft's nose is released. This action increases the aircraft's angle of attack (AOA) to facilitate takeoff. The RC aircraft rotation phase is considered to be completed in 0.5 seconds **mentioned the standard values for small and big aircraft**, during which the tires lose contact with the ground and the aircraft becomes airborne.

The specific formulation of the TO segments depends on the landing gear configuration of the aircraft. In the tricycle configuration, both the main and nose landing gears accelerate with the aircraft on the ground. Fig. 47 depicts the various velocities the aircraft attains while taking off, which are V (instantaneous speed), V_s (Stall-speed) with flaps deployed and V_{LOF} (Lift-off speed).

As per the payload requirements in the competition, the Stalling-speed (V_s) varies w.r.t various payloads. Fig. 49 depicts stall velocity curve for payloads in range [5, 6, 7, 8, 9, 10] kg (i.e 8.13, 8.57, 8.98, 9.38, 9.76 and 10.13 [m/s] respectively) **mention SAE Payload [5, 7, 9, 10]**. The estimated stall velocity (V_s) must be achieved before the aircraft goes airborne.

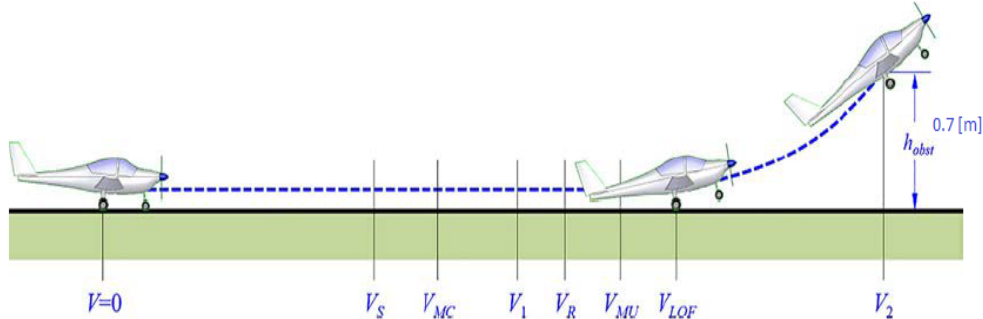


Figure 47: Takeoff Stages [2]

6.1.2 Landing (LD)

The LD maneuver of an aircraft can be divided into distinct segments, as illustrated in Fig. 48. The first segment is the Approach Distance (S_A), which is measured from the point when the aircraft is 0.7 [m] above the ground. Here the ailerons are deployed called as the flare maneuver to reduce the approach speed and control the approach angle and to facilitate a smooth touchdown on the runway.

Following the flare maneuver, the aircraft enters the Flare Distance (S_F), which extends from the initiation of the flare to the point of touchdown. After the touchdown, there is typically a brief rolling period before the brakes are applied. This rolling period is referred to as the Free-Roll Distance (S_{FR}). Finally, the Braking Distance (S_{BR}) accounts for the length of runway required for the application of braking mechanisms, and probably a reverse thrust is employed to slow the aircraft if it comes in too fast finally completely stopping the aircraft.

The primary objective of the landing analysis is to estimate the total landing distance by examining and analyzing each of these segments separately. This analysis involves applying simplified physics principles that are specific to each segment. The nomenclature used to denote these segments in the analysis aligns with the labeling shown in Fig. 48.

A temperature analysis of the landing distance was performed meaning how the landing distance varies with changing temperatures and it was also preformed in both the Sao Paulo and Linköping locations where the aircraft is generally flown for testing as well as for the competition and from Fig. 52 we can see that higher the temperature higher the landing distance also from both the location analysis we can see a longer runway is needed for the plane to land at Sao Paulo rather than Linköping.

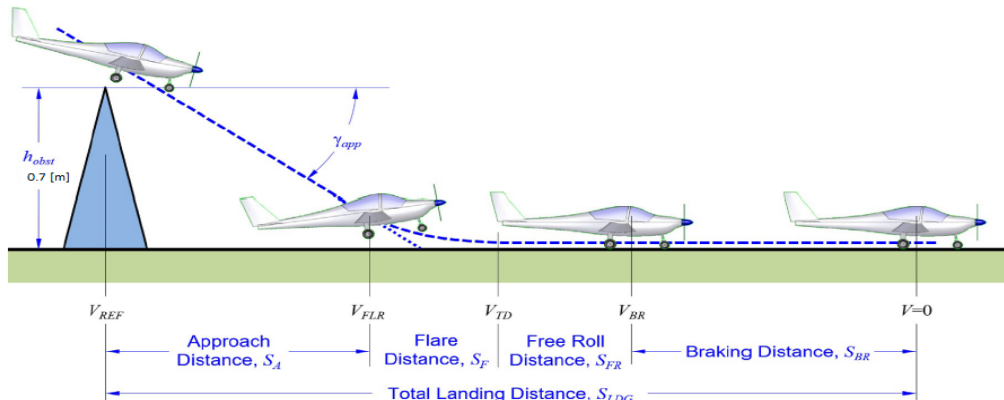


Figure 48: Landing Stages [2]

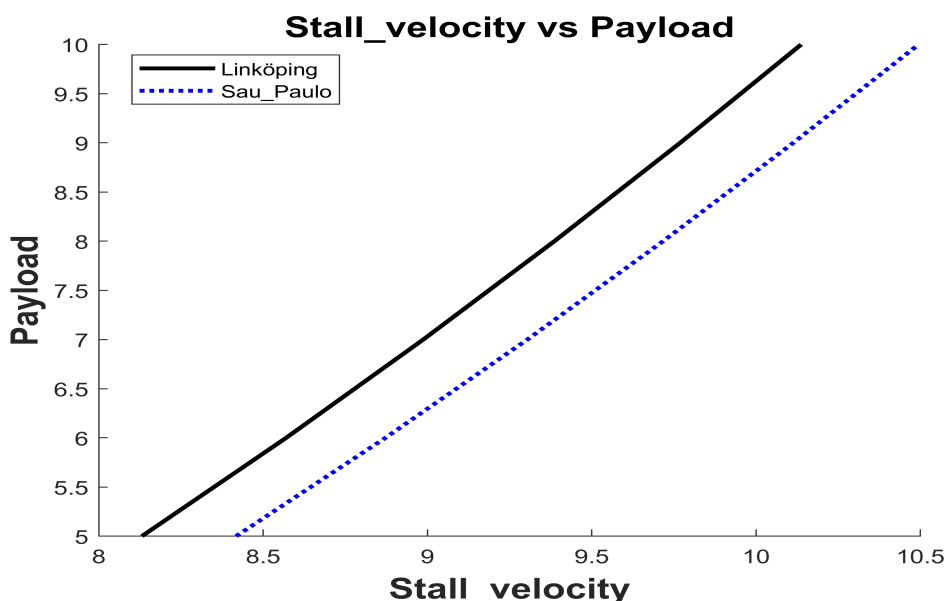


Figure 49: Stall velocity (V_s) variations in LiU and Sau Paulo (Brazil) elevations

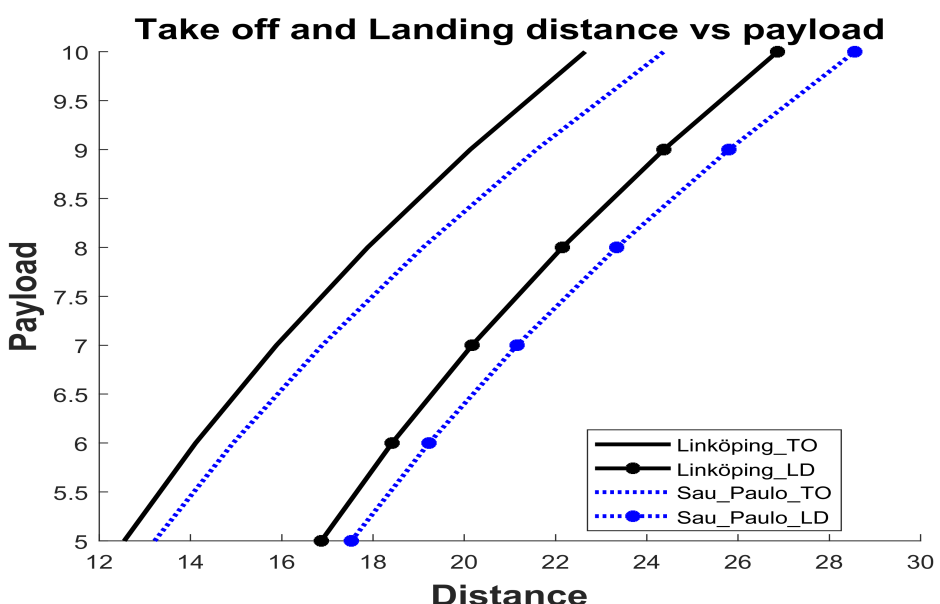


Figure 50: Take off and landing distance affected by payload increment

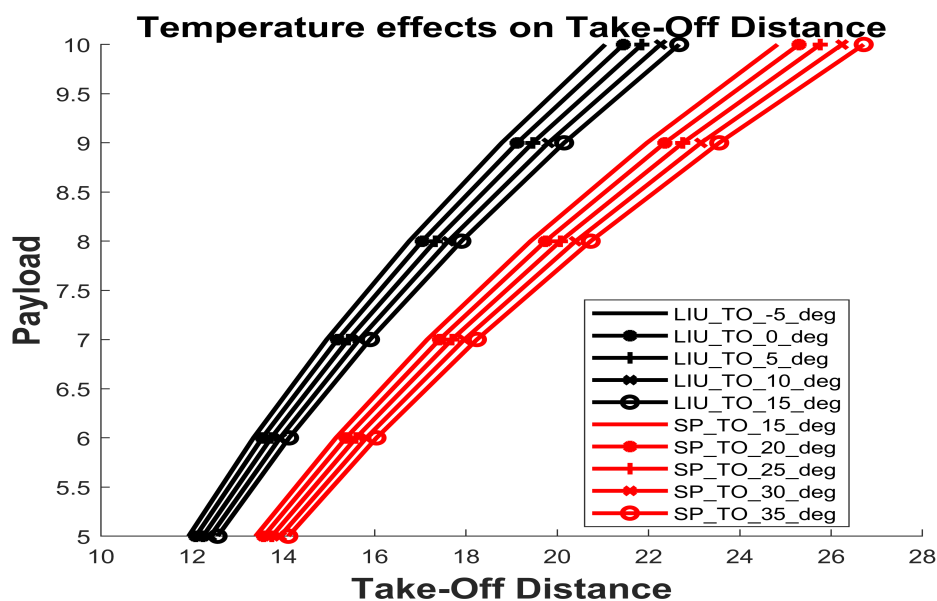


Figure 51: Temperature influence on Take distance in Linkoping and Sau Paulo

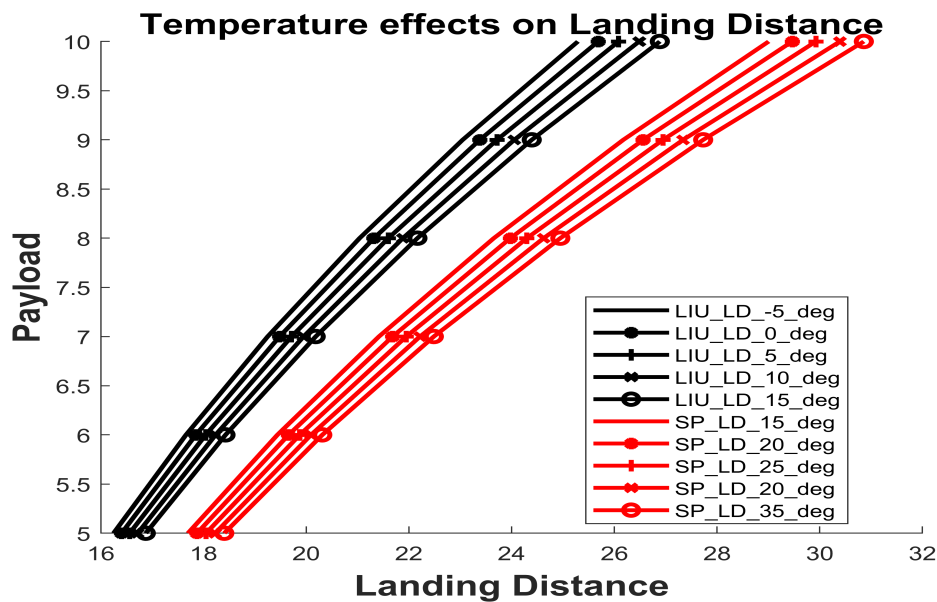


Figure 52: Temperature influence on landing distance in Linkoping and Sao Paulo

7 Stability and Control Analysis

7.1 CG Estimation

The center of gravity estimation starts with finalizing the components position and calculating the individual CG of each components and finding out the X,Y positions of each component and using the equations from [2] the CG of the aircraft can be calculated. The equations used are

$$X_{CG} = \frac{1}{W_{total}} \sum W_i x_i \quad (19)$$

$$Y_{CG} = \frac{1}{W_{total}} \sum W_i y_i \quad (20)$$

Where, W_i = Weight of Individual components,
 x_i, y_i = Locations of individual Components

Apart from the lifting surfaces the X,Y,Z CG locations are considered at half of the length and the for the lifting surfaces the CG is assumed 25% of the chord. After using Eq. [19, 20] the CG location of Aircraft is at (0.515, 0.238) which is 34.8% from the wing leading edge.

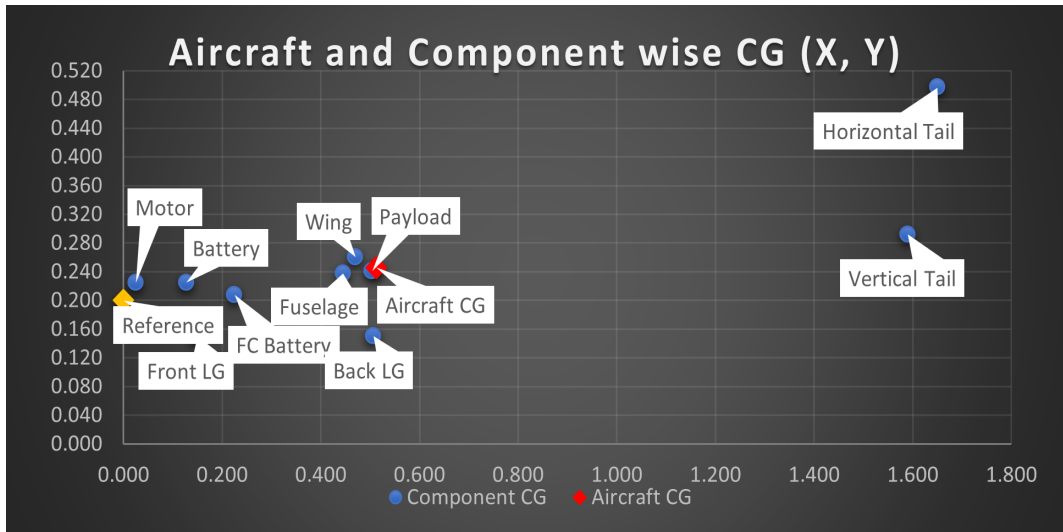


Figure 53: Individual component and Aircraft CG

From Fig. 53 we can see that the Aircraft CG corresponds to major components CG such as the Fuselage, Payload and the Wing which is ideal for the Aircraft stability in flight and also since the components are placed in front of the aircraft this generates a pitching down moment which helps flying the aircraft. Also from the figure we can see that the back landing gear CG is closer to the overall CG of the aircraft meaning the aircraft will be stable while landing. Even though many of the parts are in front of the aircraft the thick airfoil used for the horizontal stabilizer placed in inverted positioning will generate negative lift thereby balancing the aircraft.

7.2 Neutral Point (NP) and Static Margin (SM)

The aircraft's static stability is summed up by the estimation of the Neutral Point (NP) lying at some distance (X_{NP}) from a reference point (wing leading edge). For aircraft consuming fuel during flight the position of the center of gravity (CG or X_{cg}) changes from start to destination. Hence, the balance of CG plays a crucial role in regular aircraft for stability. But, the SAE competition from year i.e 2023 on-wards is emphasizing electric flights along with special **Bonus points** for the same. Therefore, the team decided to proceed with an electric aircraft.

The main source of power for an electric aircraft is the batteries that drive the propeller blade to generate the required thrust. The electrification of aircraft keeps the CG constant as no weight change happens during flight. The aerodynamic center (X_{cg}) and center (X_{NP}) are considered/assumed to be at 0.24 and 0.25 of MAC respectively. The calculation for the neutral point and the static margin is implemented in a similar way as Example 2.2 [9]. **Note: Neutral point:** is the point w.r.t to wing chord where the net pitching moment does not change with the angle of attack (α) and serves as the aft CG movement limitation. The aircraft becomes statically unstable if the CG is aft of the neutral point (NP). **Static Margin:** is the playing field for CG movement, meaning that the CG can move between its original position and NP without making the aircraft unstable. It's measured in terms of MAC.

Static Margin (SM) and Neutral Point (NP) Estimation

Parameter	Description	$X_{location}$	Unit
X_{cg}	CG location	142.295	mm
X_{np}	Neutral Point location	268.450	mm
$X_{np} - X_{cg}$	Distance between NP and CG	126.155	mm
Static Margin	% of MAC	30.22	NA

	+	-	+
Eq_Terms	X_{ac} / MAC	$fuse_term$	$tail_vol$
Team	0.2500	0.0111	0.4042
Book_eg2.2	0.2500	0.0279	0.3301

Figure 54: Comparison of term values for X_{NP} with reference

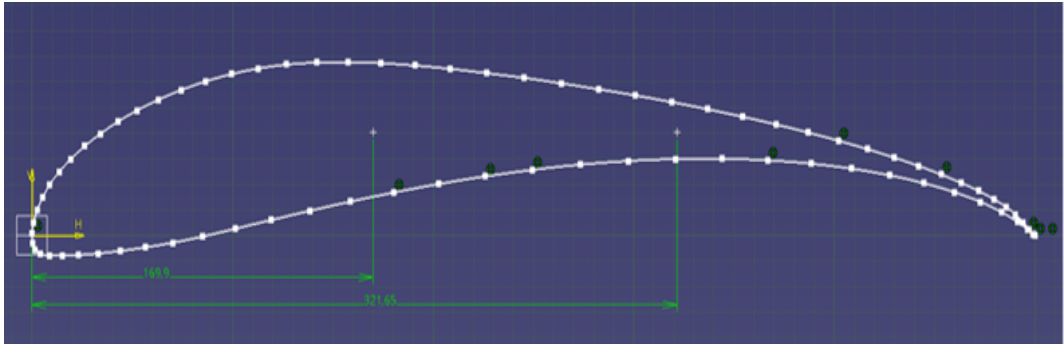


Figure 55: Aircraft CG and NP location w.r.t MAC

In the case of an electric aircraft, the CG remains constant but with possibilities of negative scenarios, it's advised to keep it within a good static margin. Based on the finalized design parameters of the conceptual design, the calculated static margin was 46.03% of MAC with a neutral point (NP) located at 70.03% of MAC, Table. [5]. These values are higher than the good range of values (Static Margin = 5% MAC, [9]). But, as the RC aircraft being designed by the team for the SAE Brazil competition has to accomplish a provided mission profile with certain constraints, these values seem reasonable leading to a large tail size and lever arm for the horizontal stabilizer to create a good pitching moment. The root cause analysis was done to estimate the potential design choices that would result in a high static margin and NP location. This resulted in the conclusion that the fuselage contribution compared to the wing in creating the pitching moment is very low (fuse_term - highlighted in yellow), Table.[54] as the S1223 airfoil has a step C_L vs α curve. Also, the horizontal stabilizer surface area combined with the lever arm length from X_{cg} was high, hence a greater static margin.

Further optimization is required for the design parameters which is intended to bring down the static margin to below 30 %.

8 Loads and Aero Elasticity

8.1 Payload and Dimension Analysis

The next step was to perform the payload dimension analysis and explore the constraints for the varying payload capacity corresponding to mission heats in the competition. The high-density material **Stainless Steel** was selected to construct the payload which is also used as weights plates in gym. The circular plates to be cut in half diametrically and placed in parallel to get the desired dimensions. Circular plates of [5 kg] cut in to half (semi-circular shape [2.5 kg each]) are the ideal choice to build the varying competition payload requirements of [5 kg, 7 kg, 10 kg] mainly, Fig. 56. The two dimensions of the payload compartment have fixed length (0.1 [m]). The varying third dimension is planned to be along the longitudinal direction to keep it under the wing. Maximum of 4 semi-circular plates ($4 * (5/2)$ [kg]) accounting for 10 [kg] payload and dimension ($0.1 \times 0.116 \times 0.1$ [m^3]). With the power constraint of 700 [W] [1] a 9 [kg] max payload was decided in order to complete the major part of the mission. The payload of the weight of (> 8 [kg]) would be finalized in the later stages, with the compartment dimension to be expendable.

Payload and Compartment Dimension Analysis					
weight [kg]	weight [kg]	length [m]	width [m]	height [m]	volume [m^3]
0.5	0.5	0.068	0.021	0.068	0.000097
Payloads combination					
5 kg	10X0.5	10	0.068	0.21	0.068
7 kg	14X0.5	14	0.068	0.294	0.068
10 kg	20X0.5	20	0.068	0.42	0.068
Mini Payload compartment dimensions					
L [m]	W(longitudinal) [m]	H [m]			
0.068	0.42	0.068			

Figure 56: Payload and payload compartment dimension analysis

8.2 Component Selection and Weight

Each selected component was chosen w.r.t the parameters provided by SAE Brazil and from trusted websites. The main components and their specifications are mentioned below,

- (1) **Battery** : The primary battery was selected with a minimum requirement of 3000 [mAh], 6 cells, and a maximum discharge of 20 C. A suitable Lithium polymer battery with a 5000 [mAh] capacity was chosen.
- (2) **Motor**: Brush-less DC motor with a motor rating of 2200 kV was selected to power the Aircraft.
- (3) **Servo** : Metal gear servos were selected for controlling the rudder, stabilizer, and ailerons.
- (4) **Flight controller** : The Matek F405-TE flight controller was selected for its built-in power-limiting capabilities, which are necessary to comply with SAE Brazil rules and to limit the power to 700 watts.
- (5) **Flight controller battery** : The Flight Controller battery was chosen with the same constraints as the primary battery except the minimum requirement being 500 [mAh] and prohibited use of LiPO batteries. A 500 [mAh] Lithium iron phosphate battery with 2 cells was chosen.
- (6) **Propeller** : Twin-blade propellers were chosen to ensure maximum efficiency at lower speeds.
- (7) **Electronic Speed controller (E.S.C.)** : Brushless E.S.C.s with a maximum current input capacity of 60 A were chosen.
- (8) **Landing Gear** : The tricycle landing gear configuration was chosen to account for the possibility of crosswinds and bouncing during touchdown. Additional components including servo rods, jumper wires, and wiring were also taken into account, and their specifications are detailed in Fig. 57, along with the specifications for the main components.

S.No	Component	Dimensions [mm]	Weight [g]	Weight [kg]
1	Battery	145 x 50 x 50	765	0.7650
2	Motor	Length : 50	83	0.0830
3	Servo	29 x 23 x 12	13.4	0.0134
4	Flight Control	33 x 20 x 11	30	0.0300
5	F.C Battery	40 x 30 x 4	40	0.0400
6	Servo Rod	260 x 1	14	0.0140
7	Jumper Wires	110 x 70 x 20	30	0.0300
8	Propeller	381 x 178	10	0.0100
9	Wiring	Length : 2000	10	0.0100
10	Electronic Speed Controller	-	63	0.0630
11	Front Landing Gear	Height : 150	120	0.1200
12	Back Landing Gear	Height : 130	240	0.2400
	Total		1458.6	1.4586

Figure 57: Component dimensions and weight

9 Structures and Structural Test

9.1 Aircraft Structures and Weight Estimation

To build an aircraft the very first step after finalizing the design and having some constraints in place is to do a Weight estimation analysis where the individual weights of each part in the aircraft are done by following several estimation methods, In this case, these statistical methods cannot be used since all the equations obtained are based on extensive research and cannot be used in estimating a Radio controlled aircraft's weight hence a weight estimation using the volume and density of each individual part used in the building of the aircraft is calculated and the individual weight of the parts are finally combined to get a rough estimate of the weight of the aircraft. The components like the Flight control system, Batteries, Motor, wires, and propeller are found individually from extensive research and computed accordingly and a miscellaneous weight of 10% was added to the final weight of the aircraft.

9.2 Lifting Surfaces

The weight of the Wing, Horizontal Tail, and Vertical Tail are found by adding the individual parts used while building the lifting surfaces the parts of the lifting surfaces are

- **Ribs** - Ribs are the Airfoils with a thickness which are used in the wing taking a shape the ribs are of 5[mm] thickness and made with airfoil **S1223**. The material used in building the Ribs is high strength Balsa Wood which has a density of 350 [kg/m³].
- **Spars** - It is the main structural object which is present span-wise at right angles to the Ribs. It is made as a half I beam since it is the best for bending loads. Two spars are used in the wing one has a height of roughly 55 [mm] which is roughly at the 25% chord of the wing and the second spar has a height of roughly 15 [mm] which is near the trailing edge of the wing since the thickness of the wing is low here a less thick spar is used here. The material used in building the Spars is high-strength Balsa Wood which has a density of 350 [kg/m³].
- **Stringers** - Stringers are generally used to connect the Wing structure to the skin of the wing, they are also present span-wise along the boundary of the wing. The width of the stringers is 6 [mm] and the height of the stringers is 4 [mm].The material used in building the Stringers is medium to high-strength Balsa Wood which has a density of 200-250 [kg/m³].
- **Skin** - The skin is the outer surface that covers much of the wing and the material used for the skin is Polythene or fiberglass which has a density of 970-1200 [kg/m³].

The weights and weight distributions of the lifting surfaces can be seen in Fig. [58, 59].

9.3 Fuselage

The fuselage is being constructed as a single hollow cuboid boom. The volume of the cuboid is calculated and multiplied by four to get the volume of the whole boom then this boom volume is multiplied by the density of medium-strength Balsa wood to get the weight off the boom. Also, the fuselage contains some strengtheners called formers which are used to increase the load-bearing capacity of the fuselage. The total number of assumed former's are 26 in which majority of those will be used under the wing to bear the load of the wing and also the weight of the payload which the aircraft needs to carry. The weight and weight distributions of the fuselage can be seen in Fig. 58.

9.4 Landing Gear

The landing gear used in the aircraft is a commercially available tricycle configuration. For the main landing gear a high-quality carbon fiber frame is used which has a weight of 135 [g] and for the front a good shock-absorbing single landing gear is used which has a weight of 70 [g] and wheels used are super light very durable wheels of weight 51 [g] each are used in the landing gear. The combined weight of the landing gear can be seen in Fig. [58, 59].

Aircraft Parts	Estimated Weights[Kg]
Vertical Stabilizer	0.1470
Payload Compartment	0.1860
Horizontal Stabilizer	0.3510
Fuselage	0.5916
Wing	0.9180
Components	1.4586
Miscellaneous	0.3652
Total Weight	4.0174

Figure 58: Weight Breakdown of Individual Components

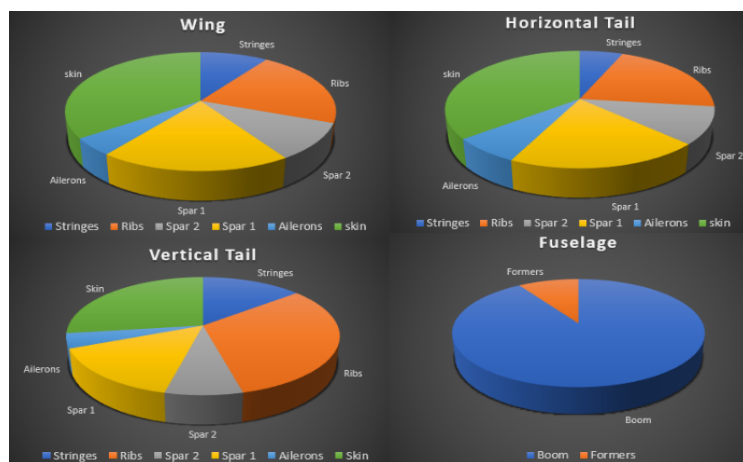


Figure 59: Individual Weight Distributions of components

10 SAE: Additional Analysis

10.1 Control Analysis

10.2 Aero Elasticity

10.3 Material Table and Structural Tests

10.4 Electrical Design and Safety Assessment

11 Conclusion and Future Scope

The final design of the aircraft exceeded the expectations and was overall deemed a success. Based on the analytical analysis the design seems very promising with high lift characteristics and really great take off and landing performance. The design also shows good power loading and wing loading within the dimensional and power constraints as per the SAE competition rules and requirements.

A good amount of work is yet to be completed by the team in order to participate and win the competition. In the upcoming months the team will focus on getting CFD analysis for the aircraft along with detailed blueprints of the aircraft's electrical components. Finally, the team under the supervision and guidance of Professor David and with the help of fellow students will likely form a student union in order to expand our group to construct the aircraft. But so far, the combined effort by the team and detailed analysis results well equips the team for upcoming challenges and skills to tackle the same.

References

- [1] 25°COMPETITION SAE BRAZIL AERODESIGN 2023;. Available from: http://arquivos.saebrasil.org.br/AeroDesign/2023/Regulamento_SAE_BRASIL_AeroDesign_2023_Rev00.pdf.
- [2] Gudmundsson DS. General Aviation Aircraft Design: Applied Methods and Procedures. 2nd ed. Elsevier Science; 2021.
- [3] Remote Control Aircraft for the SAE Aero Design West Competition;. Available from: https://web.wpi.edu/Pubs/E-project/Available/E-project-042418-161050/unrestricted/SAE_MQP_Report_Final.pdf.
- [4] SAE BRAZIL AERODESIGN COMPETITION;. Available from: <https://mme.fiu.edu/wp-content/uploads/2014/11/2014Fall-BS-Thesis-T06-SAE-Brasil-Aero.pdf>.
- [5] SAE AERO DESIGN WEST “THE WRIGHT STUFF”;,. Available from: <http://edge.rit.edu/edge/P16121/public/Benchmarking/Reports/UGRADSReport.pdf>.
- [6] Raymer DP. Aircraft Design: A Conceptual Approach. 4th ed. AIAA education series. Washington, D.C.: American Institute of Aeronautics and Astronautics; 2006. Available from: <https://login.e.bibl.liu.se/login?url=https://search.ebscohost.com/login.aspx?direct=true&db=cat00115a&AN=1kp.457154&site=eds-live&scope=site>.
- [7] Advantages and disadvantages of straight wing, swept wing, forward swept wing, variable swept wing, delta wing, canard wing;,. Available from: <https://inf.news/ne/military/fddff14e3aae6646693fe471e90718c2b.html>.
- [8] Straight Wing Advantages | Wing Design;,. Available from: <https://aviationinfo.net/straight-wing-advantages-wing-design/>.
- [9] Nelson DRC. Flight Stability and Automatic Control. 2nd ed. McGraw Hill; 1998.